Climate4you update January 2015
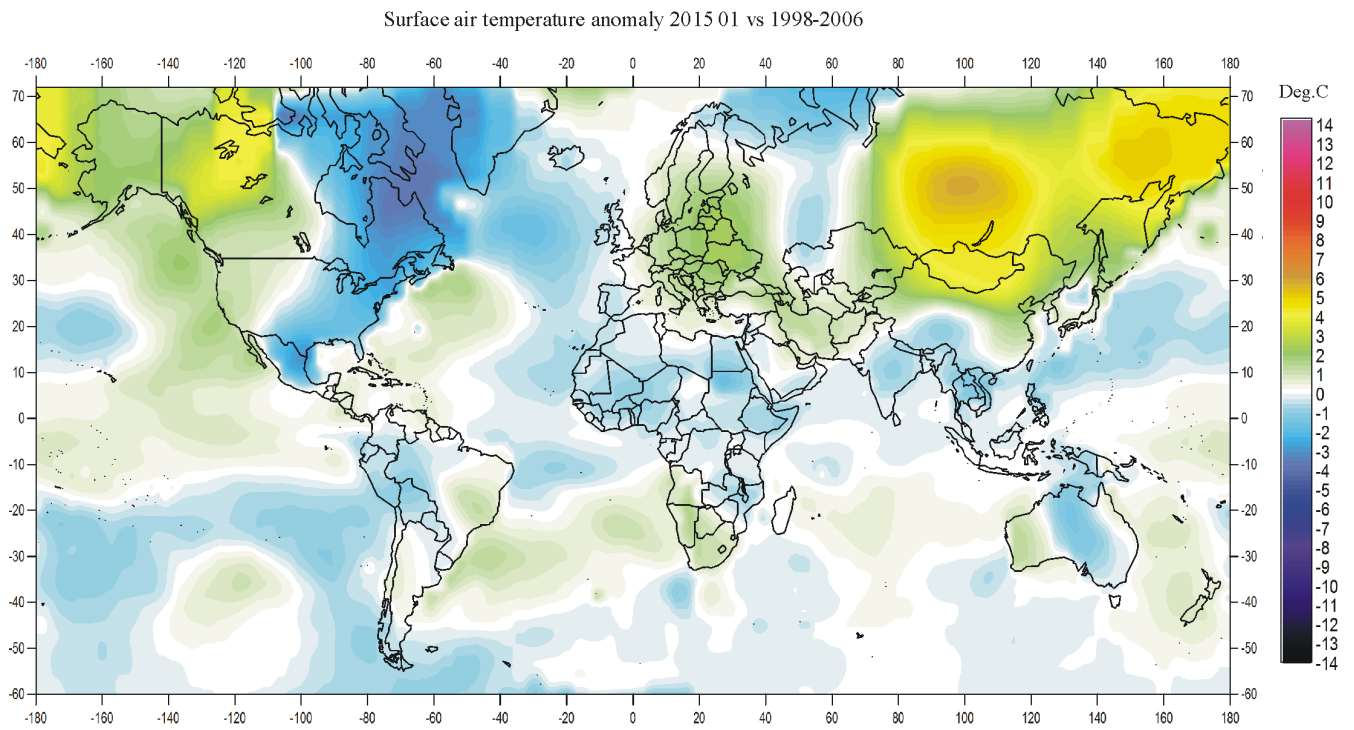

Contents:

All diagrams in this newsletter as well as links to the original data are available on www.climate4you.com

January 2015 global surface air temperature overview

Surface air temperature anomaly 2015 01 vs 1998-2006

Air temperature 2015 01 versus average 1998-2006
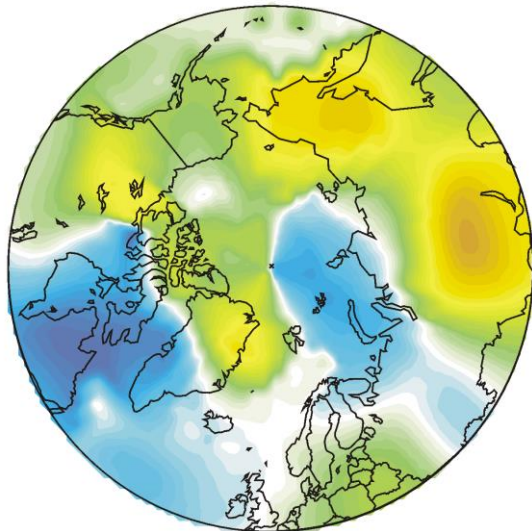
Air temperature 2015 01 versus average 1998-2006
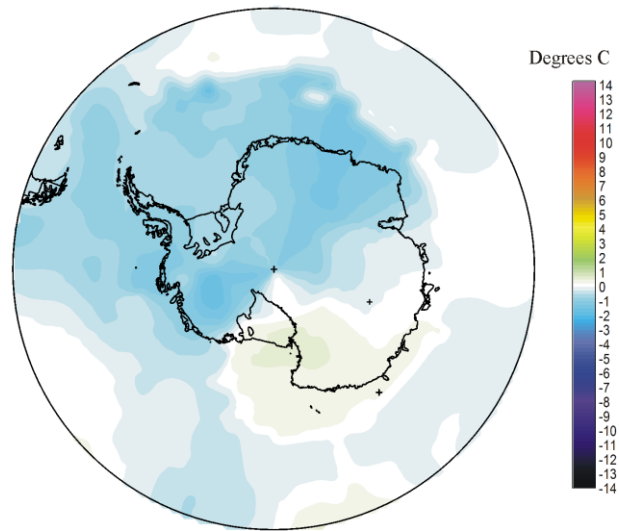
January 2015 surface air temperature compared to the 1998-2006 average. Green-yellow-red colours indicate areas with higher temperature than the 1998-2006 average, while blue colours indicate lower than average temperatures. Data source: Goddard Institute for Space Studies (GISS).

General: This newsletter contains graphs showing a selection of key meteorological variables for the past month. *All temperatures are given in degrees Celsius*.

In the above maps showing the geographical pattern of surface air temperatures, *the period 1998-2006 is used as reference period*. The reason for comparing with this recent period instead of the official WMO 'normal' period 1961-1990, is that the latter period is affected by the cold period 1945-1980. Most comparisons with such a low average value will therefore appear as warm, and it will be difficult to decide if modern surface air temperatures are increasing or decreasing. Comparing with a more recent period overcomes this problem.

In addition to the above consideration, the recent temperature development suggests that the time window 1998-2006 may roughly represent a global temperature peak (see, e.g., p. 4-6). However, it might be argued that the time interval 1999-2006 or 2000-2006 would better represent a possible temperature peak period. However, by starting in 1999 (or 2000) the cold La Niña period 1999-2000 would result in a unrealistic low reference temperature by excluding the previous warm El Niño in 1998. These two opposite phenomena must be considered together to obtain a representative reference average, and this why the year 1998 is included in the adopted reference period.

Finally, the GISS temperature data used for preparing the above diagrams show a pronounced temporal instability for data before 1998 (see p. 7). Any comparison with the WMO 'normal' period 1961-1990 is therefore influenced by monthly changing values for the so-called 'normal' period, which is therefore not suited as reference.

In the other diagrams in this newsletter *the thin line represents the monthly global average value*, and *the thick line indicate a simple running average*, in most cases a simple moving 37-month average, nearly corresponding to a three-year average. The 37-month average is calculated from values covering a range from 18 month before to 18 months after, with equal weight for every month.

The year 1979 has been chosen as starting point in many diagrams, as this roughly corresponds to both the beginning of satellite observations and the onset of the late 20th century warming period. However, several of the records have a much longer record length, which may be inspected in greater detail on www.Climate4you.com.

January 2015 global surface air temperatures

General: In general, the global air temperature was near the 1998-2006 average.

The Northern Hemisphere was characterised by marked regional air temperature contrasts, as usual. Eastern North America and southern Greenland had temperatures below the 1998-2006 average, as had the northern part of the Nordic Countries and NW Russia. Siberia, Alaska and western Canada had above average temperatures. The Arctic was mainly above average temperature, but with the Svalbard-Russia sector being colder. Temperatures across the Arctic Ocean are, however, very sensitive to the GISS interpolation technique, and the pattern displayed in the map on page 1 should not be over interpreted.

Near the Equator temperatures conditions were generally near or somewhat below the 1998-2006 average, but with parts of the Pacific being relatively warm.

The Southern Hemisphere temperatures were mainly near or below average 1998-2006 conditions. The Antarctic continent had generally below average 1998-2006 temperatures.

3

Lower troposphere temperature from satellites, updated to January 2015
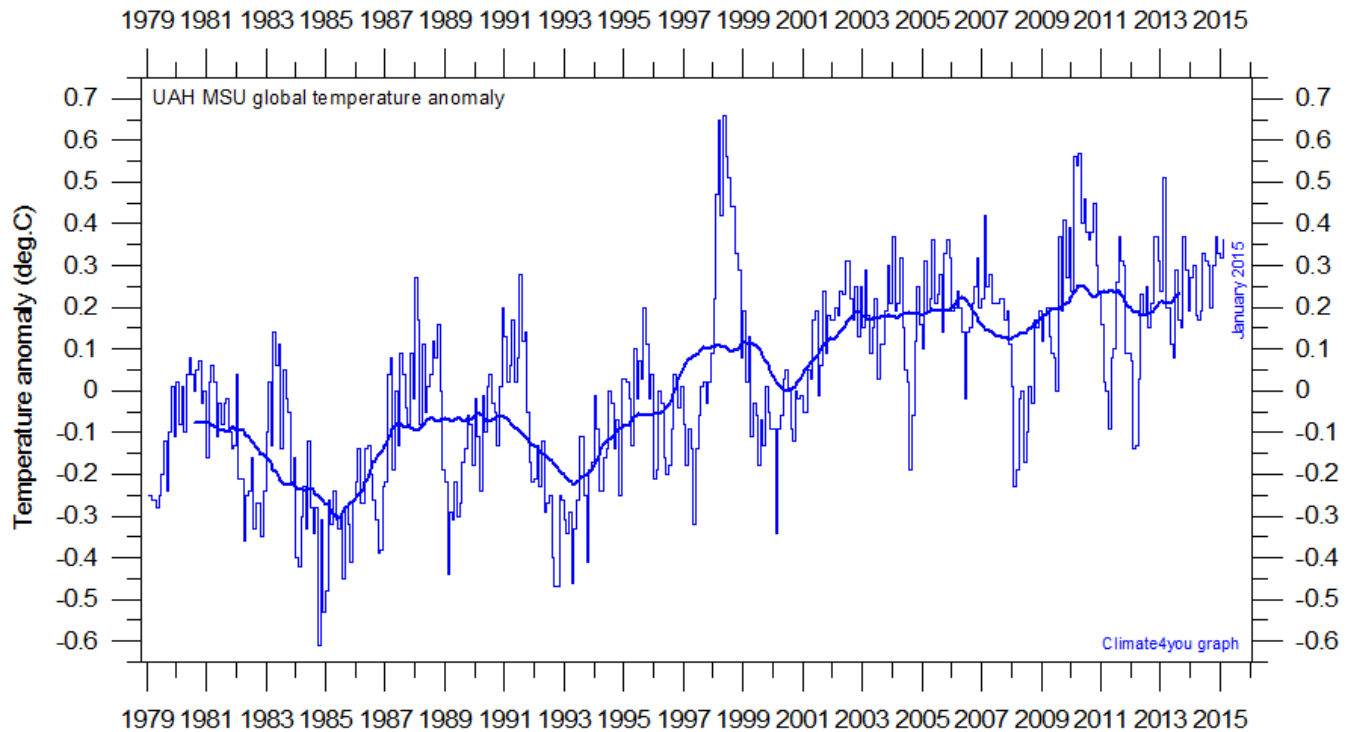
Global monthly average lower troposphere temperature (thin line) since 1979 according to University of Alabama at Huntsville, USA. The thick line is the simple running 37-month average.
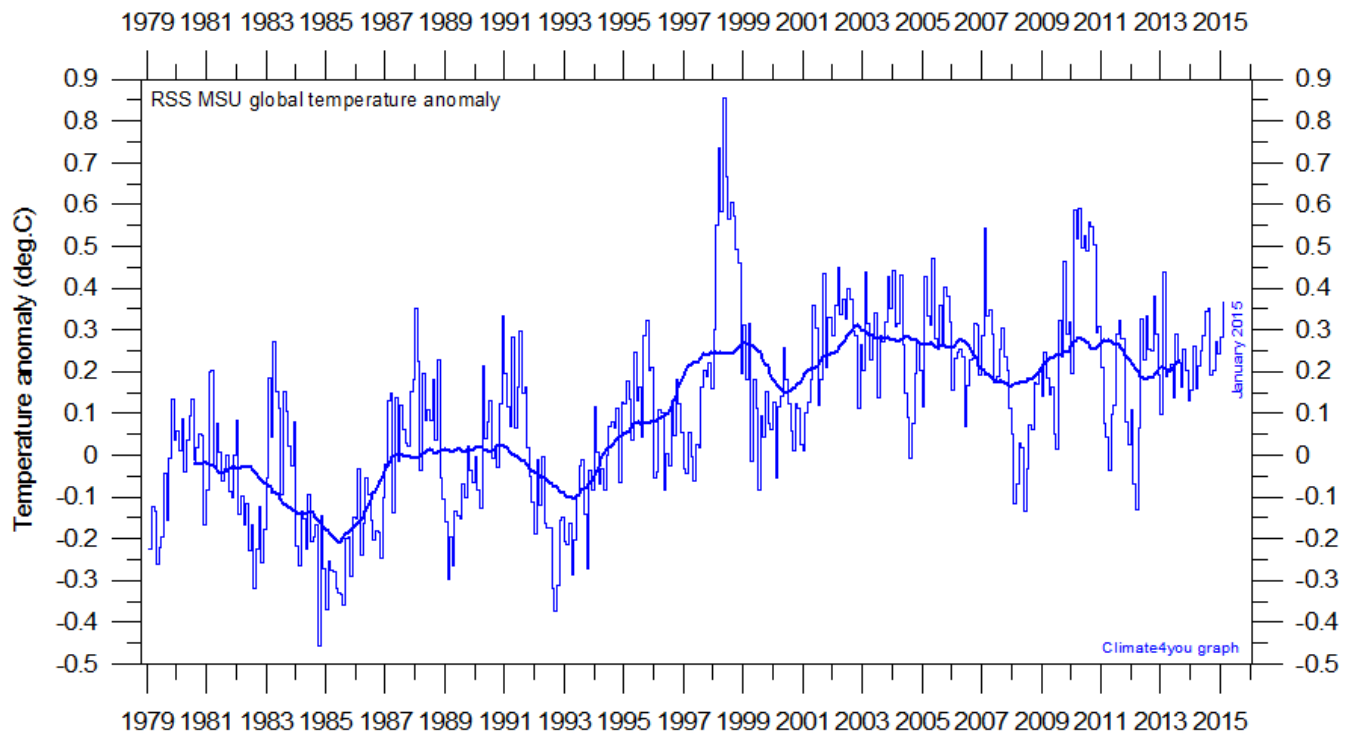
Global monthly average lower troposphere temperature (thin line) since 1979 according to according to Remote Sensing Systems (RSS), USA. The thick line is the simple running 37-month average.

Global surface air temperature, updated to January 2015
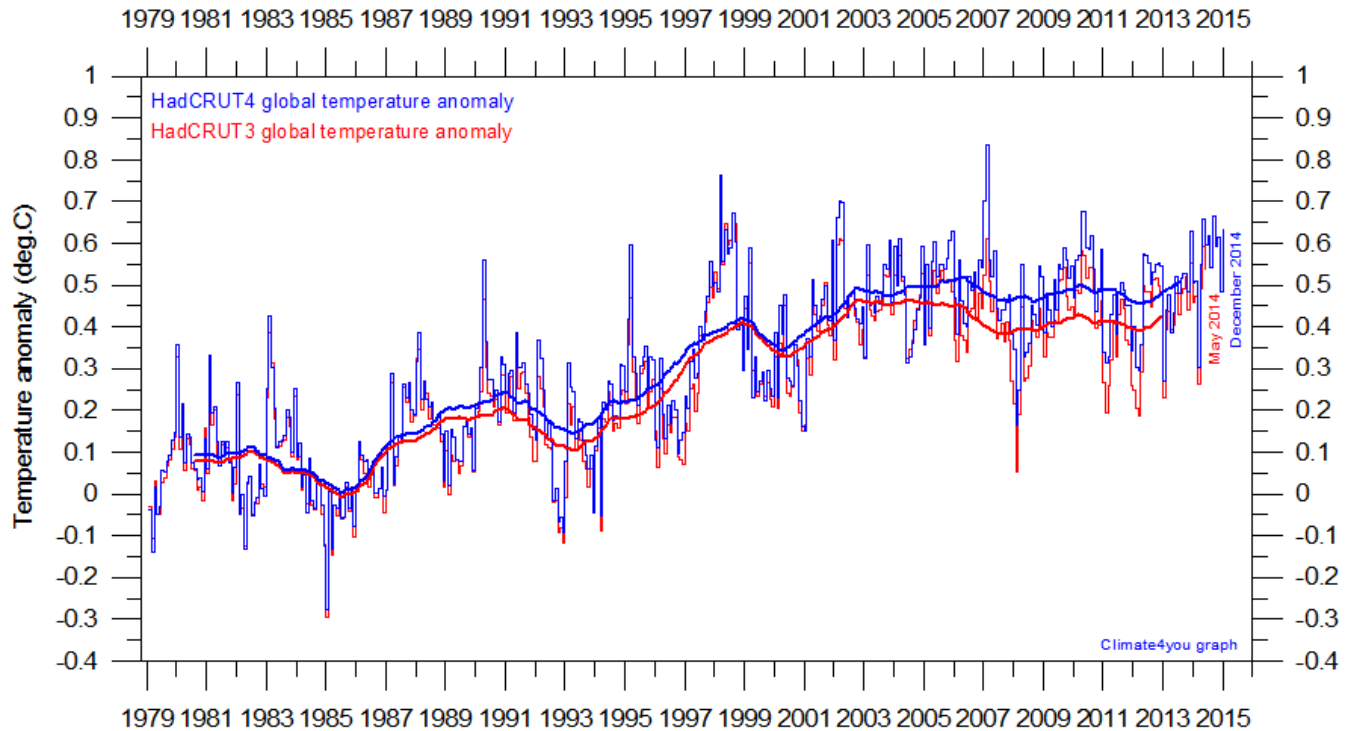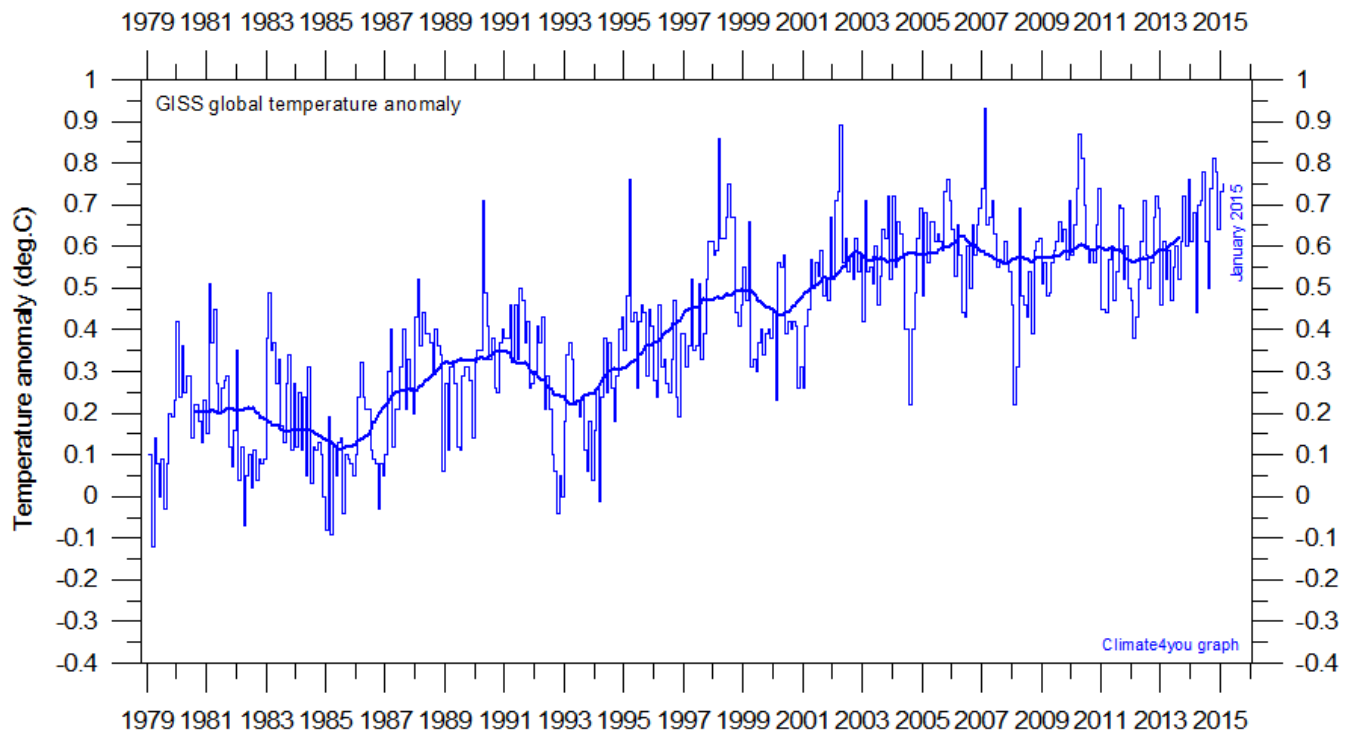

Global monthly average surface air temperature (thin line) since 1979 according to according to the Hadley Centre for Climate Prediction and Research and the University of East Anglia's Climatic Research Unit (CRU), UK. The thick line is the simple running 37-month average. Version HadCRUT4 (blue) is now replacing HadCRUT3 (red). Please note that this diagram is not yet updated beyond December 2014.

Global monthly average surface air temperature (thin line) since 1979 according to according to the Goddard Institute for Space Studies (GISS), at Columbia University, New York City, USA. The thick line is the simple running 37-month average.
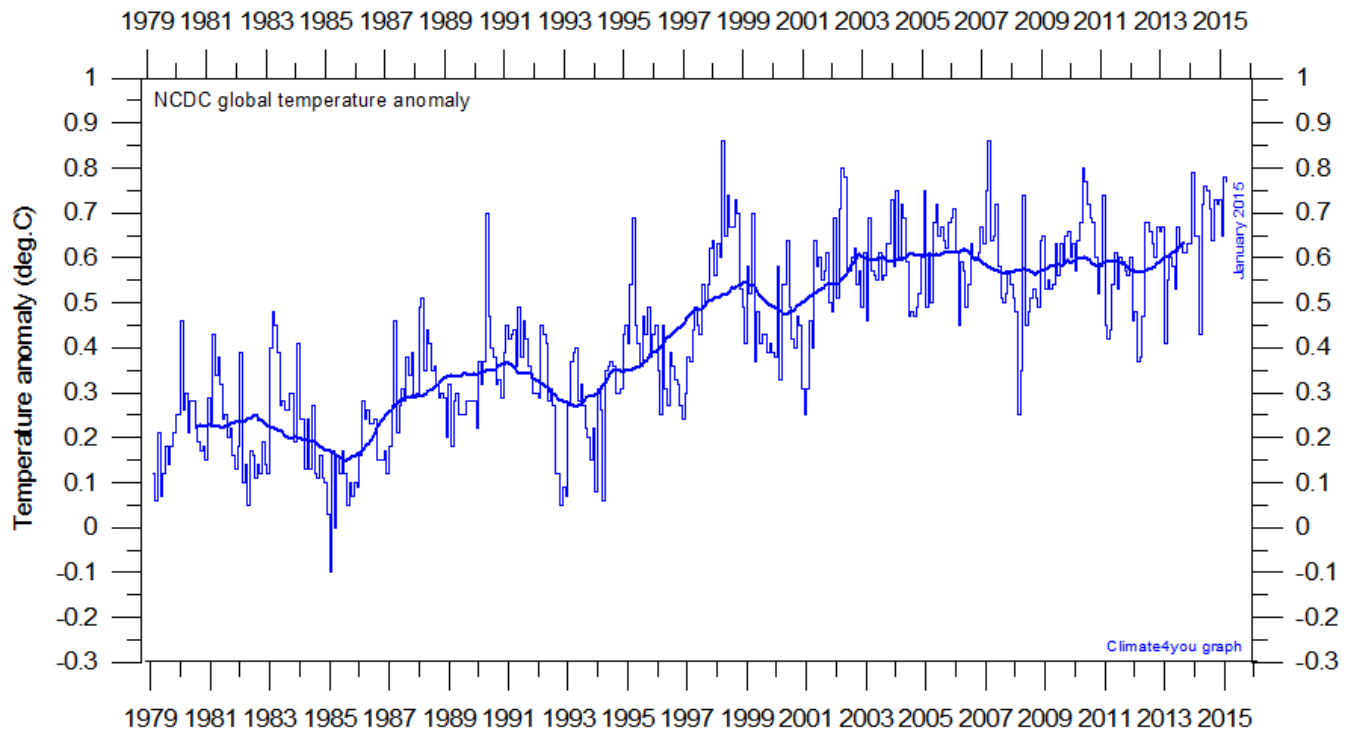
Global monthly average surface air temperature since 1979 according to according to the [National Climatic Data Center](#) (NCDC), USA. The thick line is the simple running 37-month average.

A note on data record stability:

 All the above temperature estimates display changes when one compare with previous monthly data sets, not only for the most recent months as a result of supplementary data being added, but actually for all months back to the very beginning of the records, more than 100 years ago. Presumably this reflects recognition of errors, changes in the averaging procedure, and the influence of other unknown phenomena.

None of the temperature records are entirely stable over time (since 2008). The two surface air temperature records, NCDC and GISS, show apparent systematic changes over time. This is exemplified the diagram on the following page showing the changes since May 2008 in the NCDC global surface temperature record for January 1915 and January 2000, illustrating how the difference between the early and late part of the temperature records gradually is growing by administrative adjustments.

You can find more on the issue of lack of temporal stability on [www.climate4you](#) (go to: *Global Temperature*, followed by *Temporal Stability*).

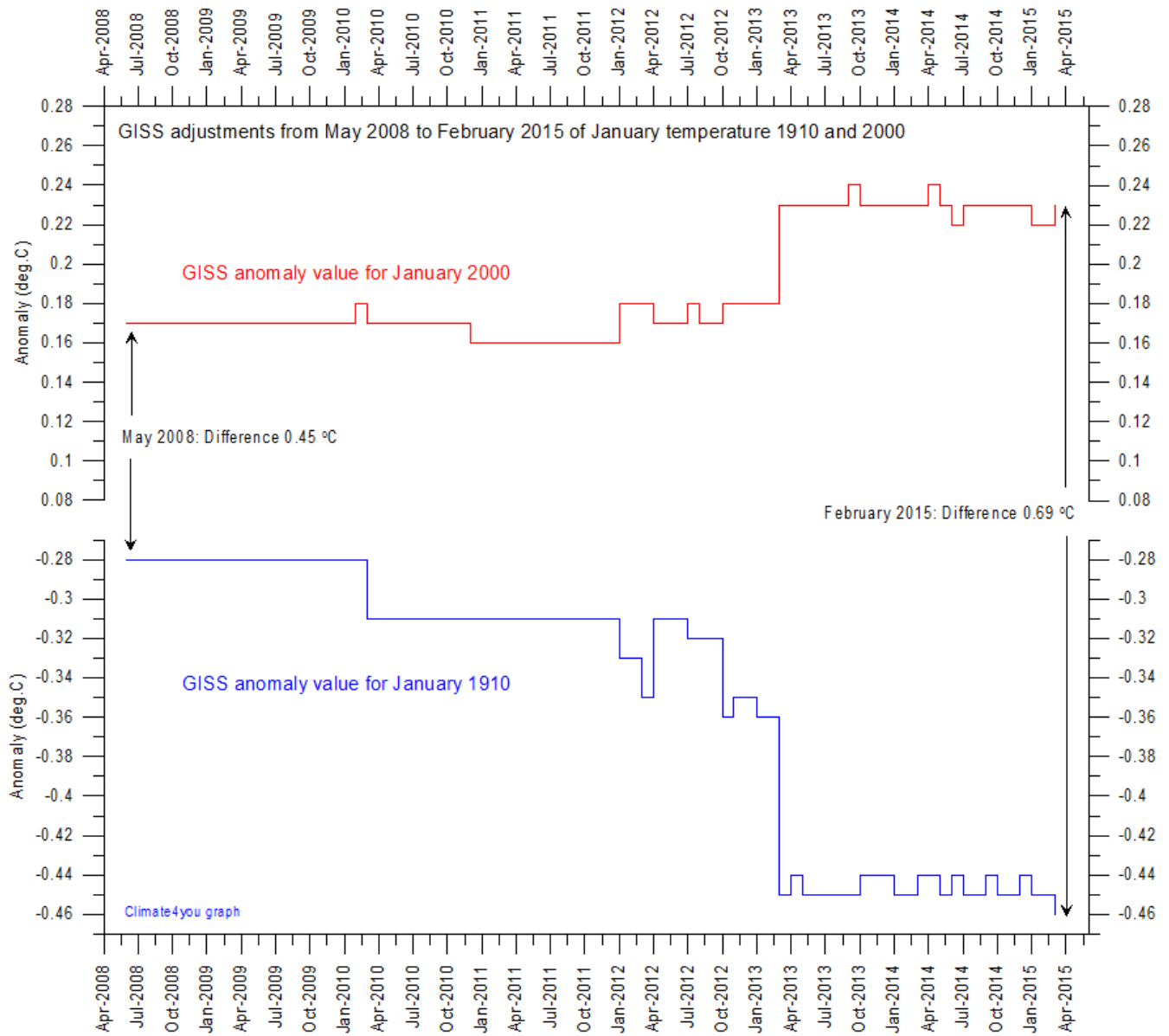*Diagram showing the adjustment made since May 2008 by the [Goddard Institute for Space Studies](#) (GISS) in anomaly values for the months January 1910 and January 2000.*

Note: The administrative upsurge of the temperature increase between January 1915 and January 2000 has grown from 0.45 (May 2008) to 0.69 °C (January 2015), representing no less than an about **53%** administrative temperature increase over this period.

Global air temperature linear trends updated to December 2014

Diagram showing the latest 5, 10, 20 and 30 yr linear annual global temperature trend, calculated as the slope of the linear regression line through the data points, for two satellite-based temperature estimates (UAH MSU and RSS MSU). Last month included in analysis: December 2014.
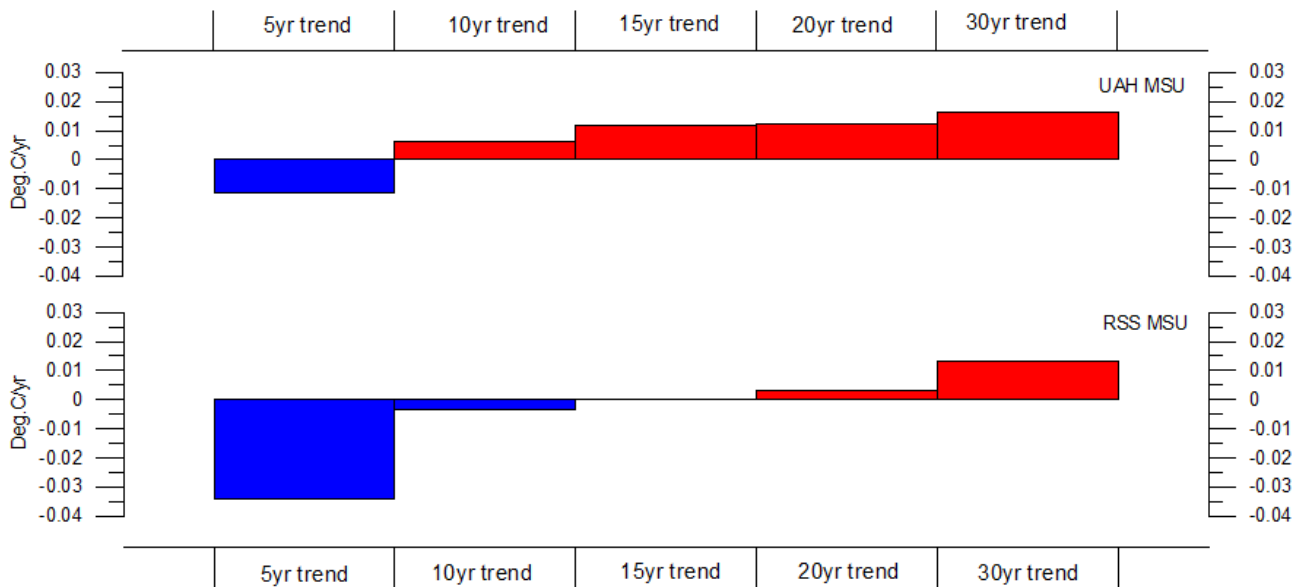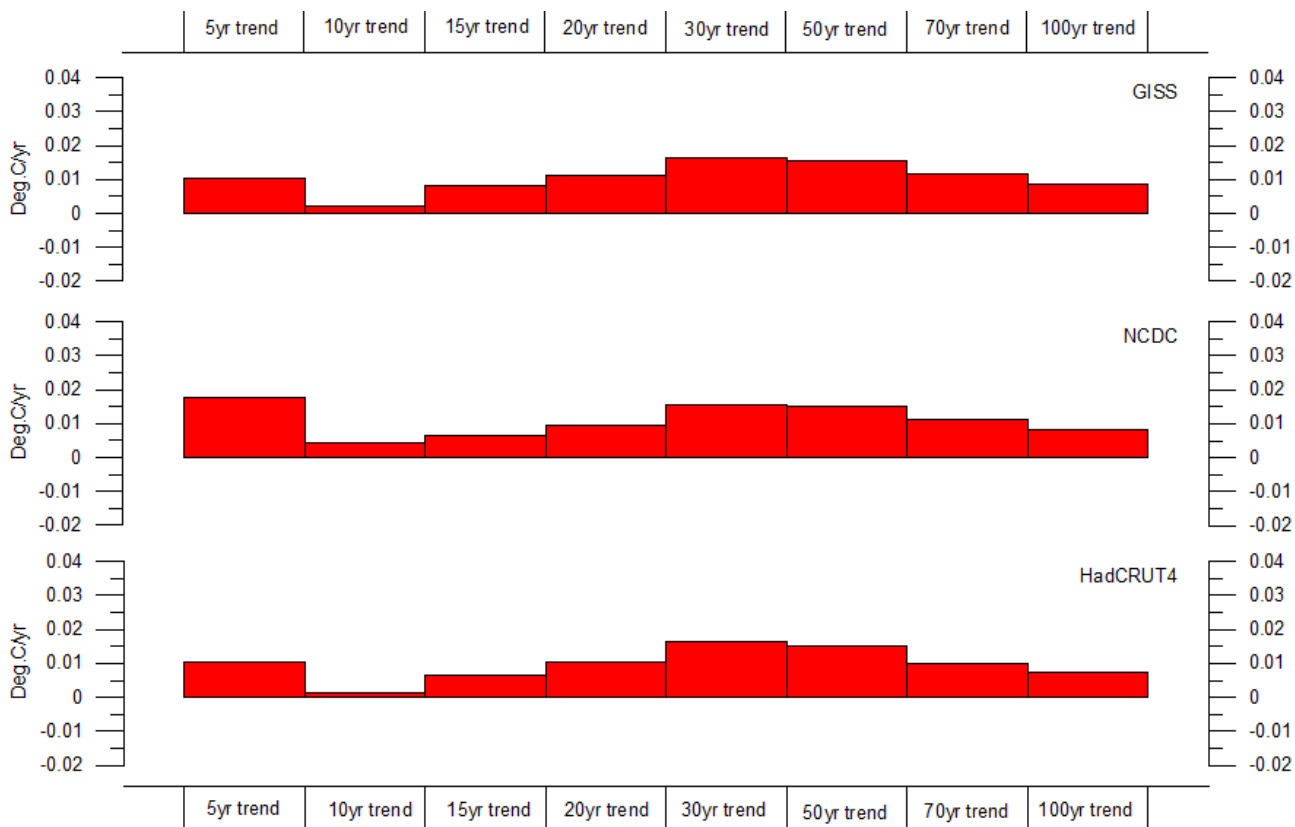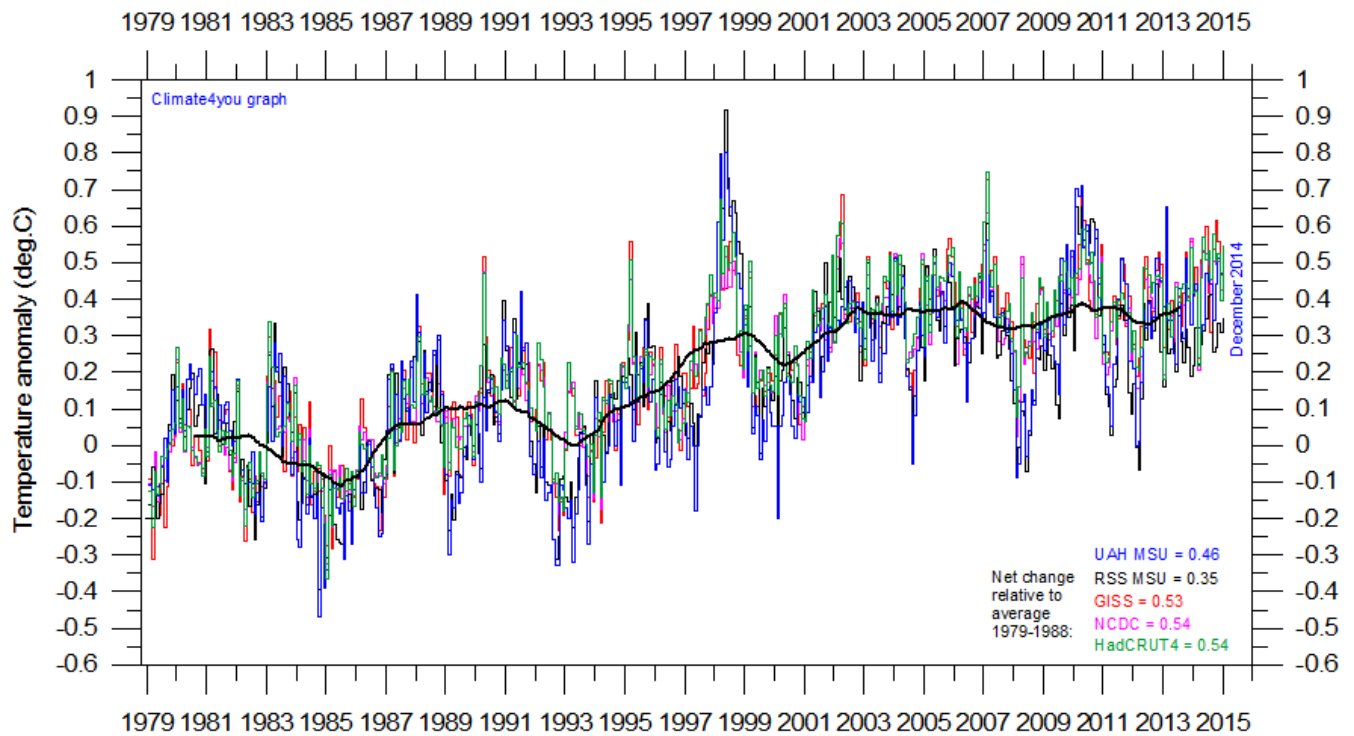
Diagram showing the latest 5, 10, 20, 30, 50, 70 and 100 year linear annual global temperature trend, calculated as the slope of the linear regression line through the data points, for three surface-based temperature estimates (GISS, NCDC and HadCRUT4). Last month included in all analyses: December 2014.

All in one, updated to December 2014

Superimposed plot of all five global monthly temperature estimates. As the base period differs for the individual temperature estimates, they have all been normalised by comparing with the average value of the initial 120 months (10 years) from January 1979 to December 1988. The heavy black line represents the simple running 37 month (c. 3 year) mean of the average of all five temperature records. The numbers shown in the lower right corner represent the temperature anomaly relative to the individual 1979-1988 averages.

9

It should be kept in mind that satellite- and surface-based temperature estimates are derived from different types of measurements, and that comparing them directly as done in the diagram above therefore may be somewhat problematical. However, as both types of estimate often are discussed together, the above diagram may nevertheless be of some interest. In fact, the different types of temperature estimates appear to agree quite well as to the overall temperature variations on a 2-3 year scale, although on a shorter time scale there are often considerable differences between the individual records.

All five global temperature estimates presently show an overall stagnation, at least since 2002. There has been no increase in global air temperature since 1998, which however was affected by the oceanographic El Niño event. This stagnation does not exclude the possibility that global temperatures will begin to increase again later. On the other hand, it also remain a possibility that Earth just now is passing a temperature peak, and that global temperatures will begin to decrease during the coming years. Time will show which of these two possibilities is correct.

Global sea surface temperature, updated to January 2015

NOAA/NWS/NCEP/EMC Marine Modeling and Analysis Branch

RTG_SST Anomaly (0.5 deg X 0.5 deg) for 29 Jan 2015

22:52:40 THU JAN 29 2015

degrees C
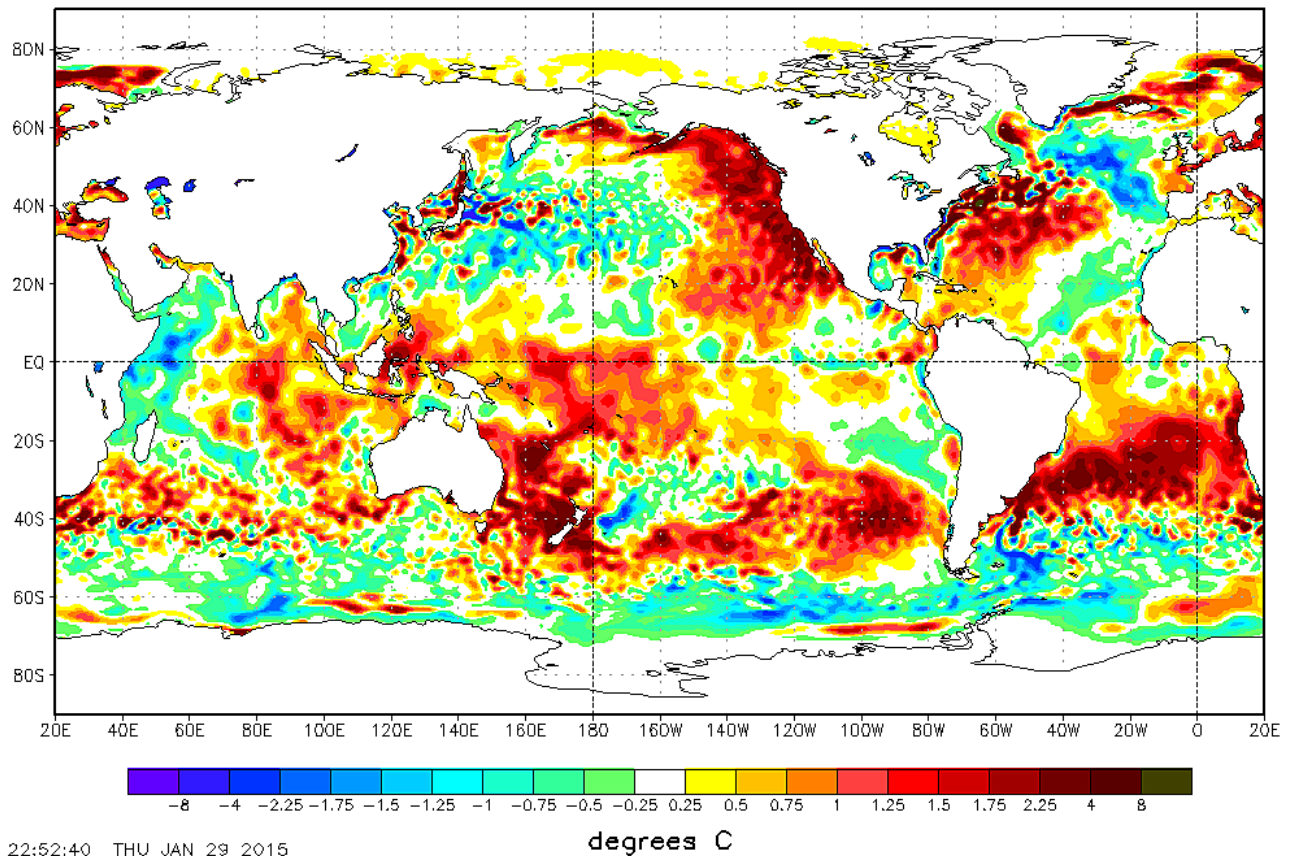
Sea surface temperature anomaly on 29 January 2015. Map source: National Centers for Environmental Prediction (NOAA).

Because of the large surface areas near Equator, the temperature of the surface water in these regions is especially important for the global atmospheric temperature (p.4-6).

Relatively warm water is dominating the Pacific Ocean and Indian Ocean near the Equator, and is influencing global air temperatures now and in the months to come.

The significance of any such short-term cooling or warming reflected in air temperatures should not be over stated. Whenever Earth experiences cold La Niña or warm El Niño episodes (Pacific Ocean) major heat exchanges takes place between the Pacific Ocean and the atmosphere above, eventually showing up in estimates of the global air temperature.

However, this does not reflect similar changes in the total heat content of the atmosphere-ocean system. In fact, global net changes can be small and such heat exchanges may mainly reflect redistribution of energy between ocean and atmosphere. What matters is the overall temperature development when seen over a number of years.
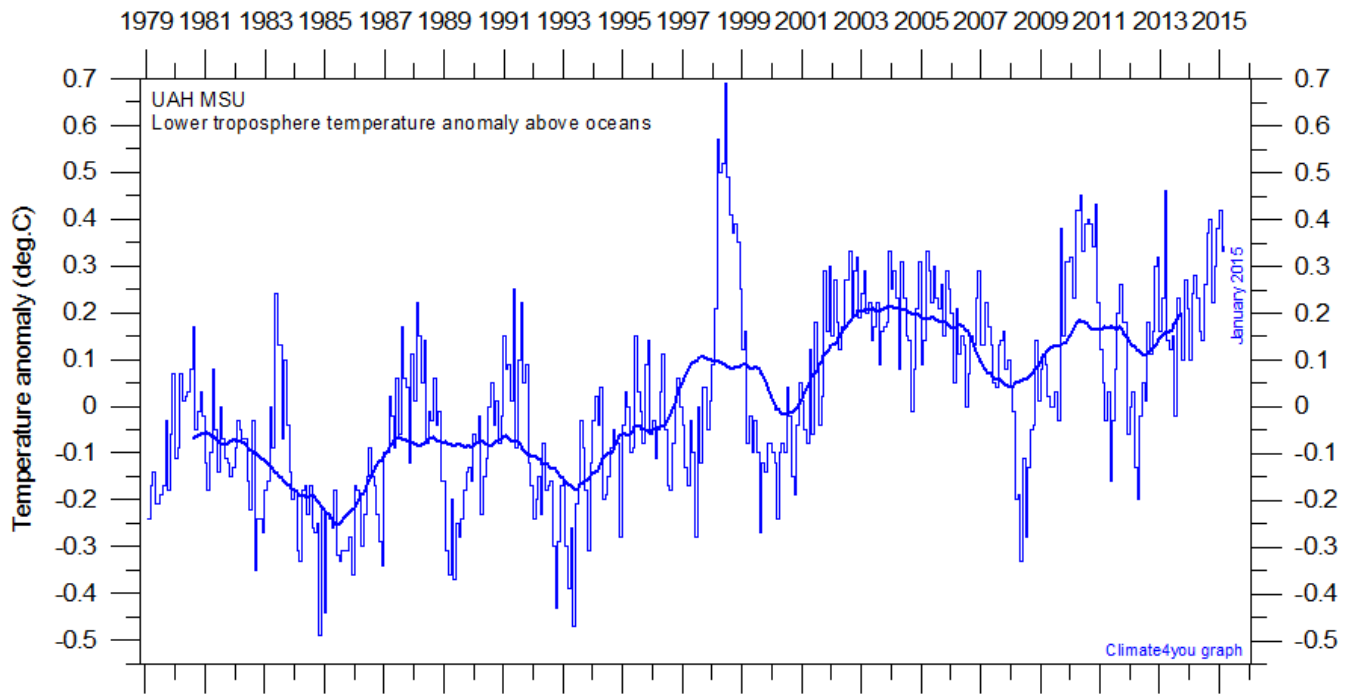
Global monthly average lower troposphere temperature over oceans (thin line) since 1979 according to [University of Alabama](#) at Huntsville, USA. The thick line is the simple running 37 month average.
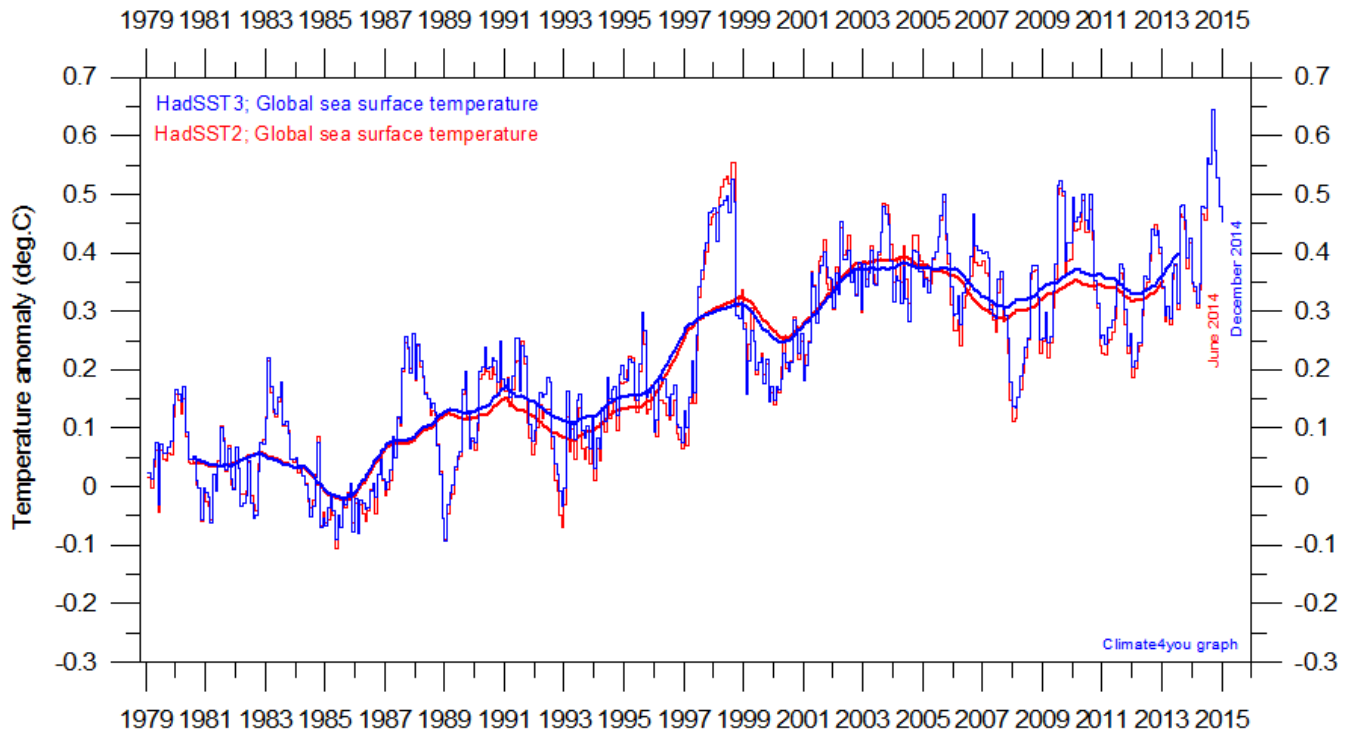
Global monthly average sea surface temperature since 1979 according to University of East Anglia's [Climatic Research Unit](#) ([CRU](#)), UK. Base period: 1961-1990. The thick line is the simple running 37-month average. Please note that this diagram is not updated beyond December 2014.
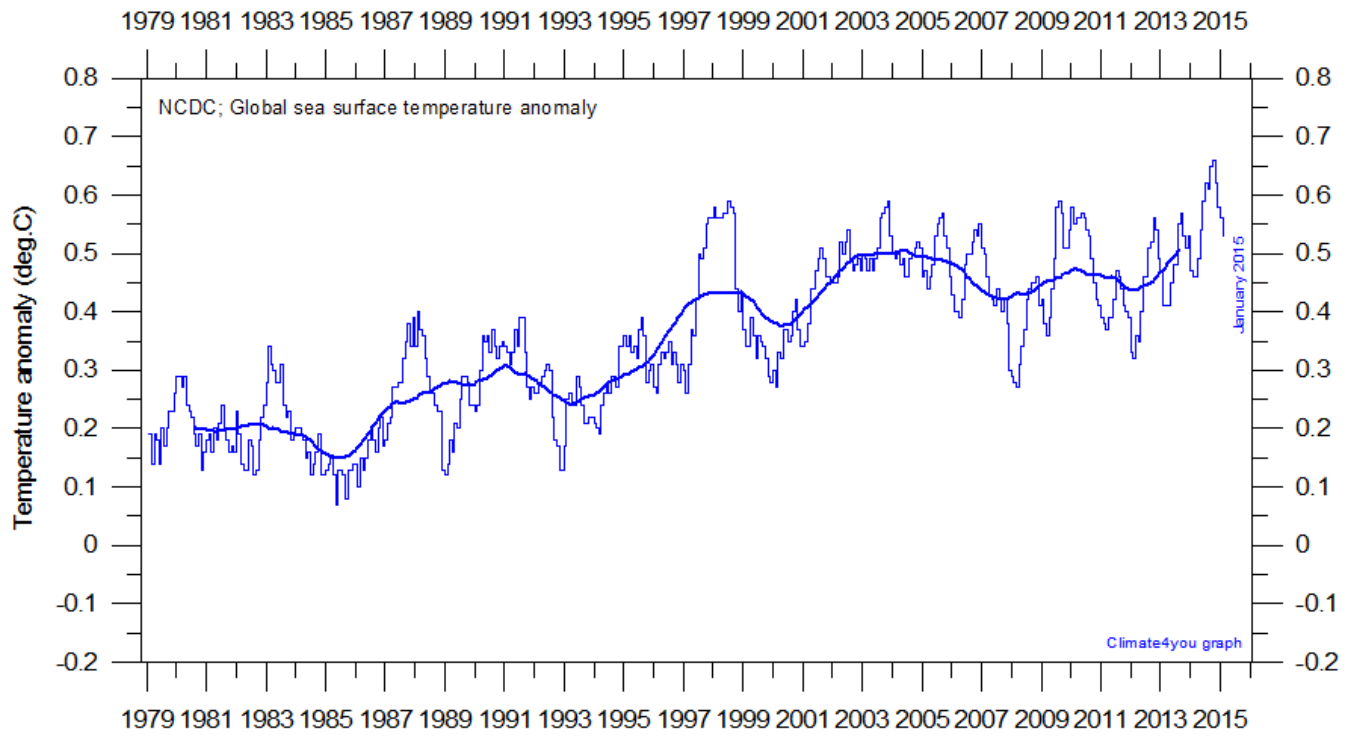
Global monthly average sea surface temperature since 1979 according to the National Climatic Data Center (NCDC), USA. Base period: 1901-2000. The thick line is the simple running 37-month average.

Ocean heat content uppermost 100 and 700 m, updated to December 2014
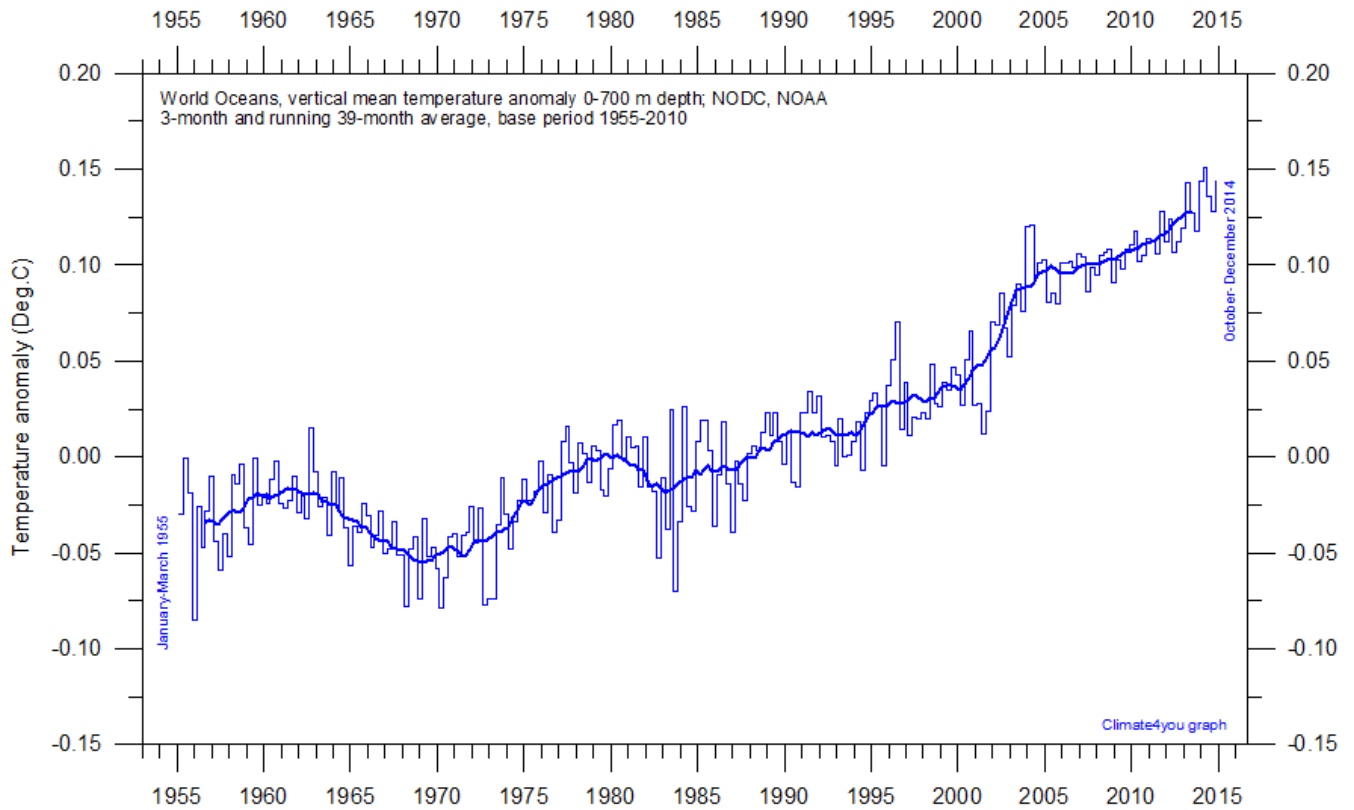
Global monthly heat content anomaly (GJ/m2) in the uppermost 700 m of the oceans since January 1955. Data source: National Oceanographic Data Center(NODC).
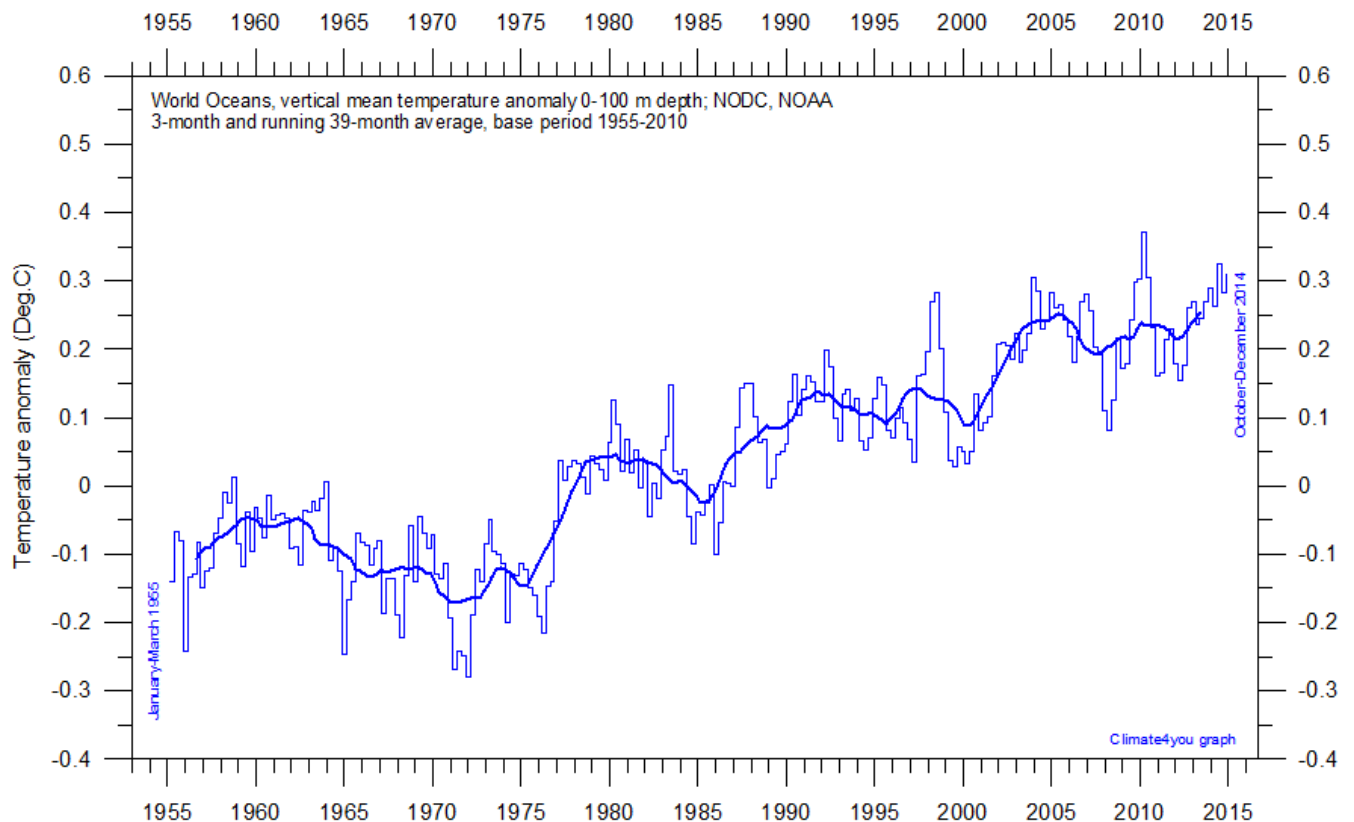
World Oceans vertical average temperature 0-100 m depth since 1955. The thin line indicate 3-month values, and the thick line represents the simple running 39-month (c. 3 year) average. Data source: NOAA National Oceanographic Data Center (NODC). Base period 1955-2010.

Pacific Ocean vertical average temperature 0-100 m depth since 1955. The thin line indicate 3-month values, and the thick line represents the simple running 39-month (c. 3 year) average. Data source: [NOAA National Oceanographic Data Center](#) (NODC). Base period 1955-2010.
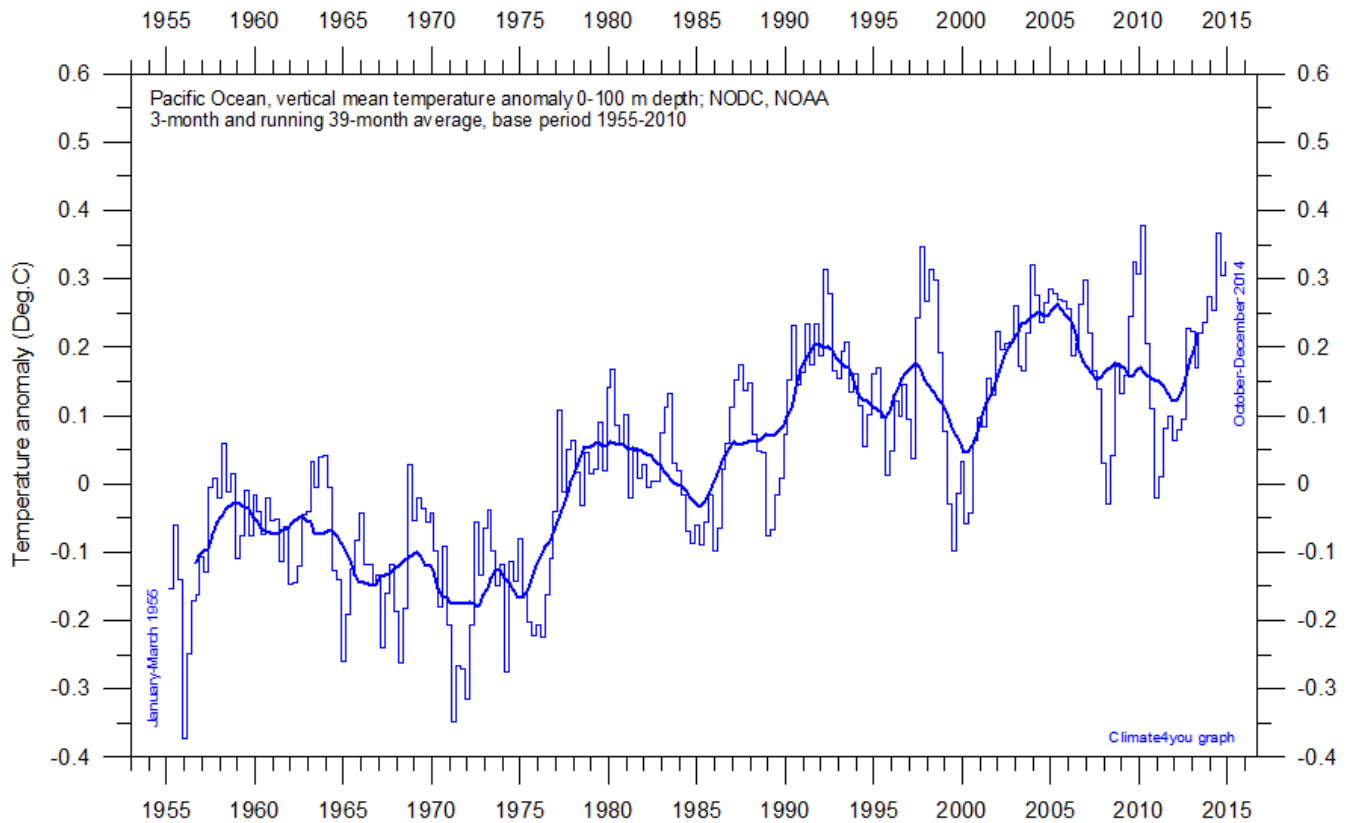
Atlantic Ocean vertical average temperature 0-100 m depth since 1955. The thin line indicate 3-month values, and the thick line represents the simple running 39-month (c. 3 year) average. Data source: [NOAA National Oceanographic Data Center](#) (NODC). Base period 1955-2010.
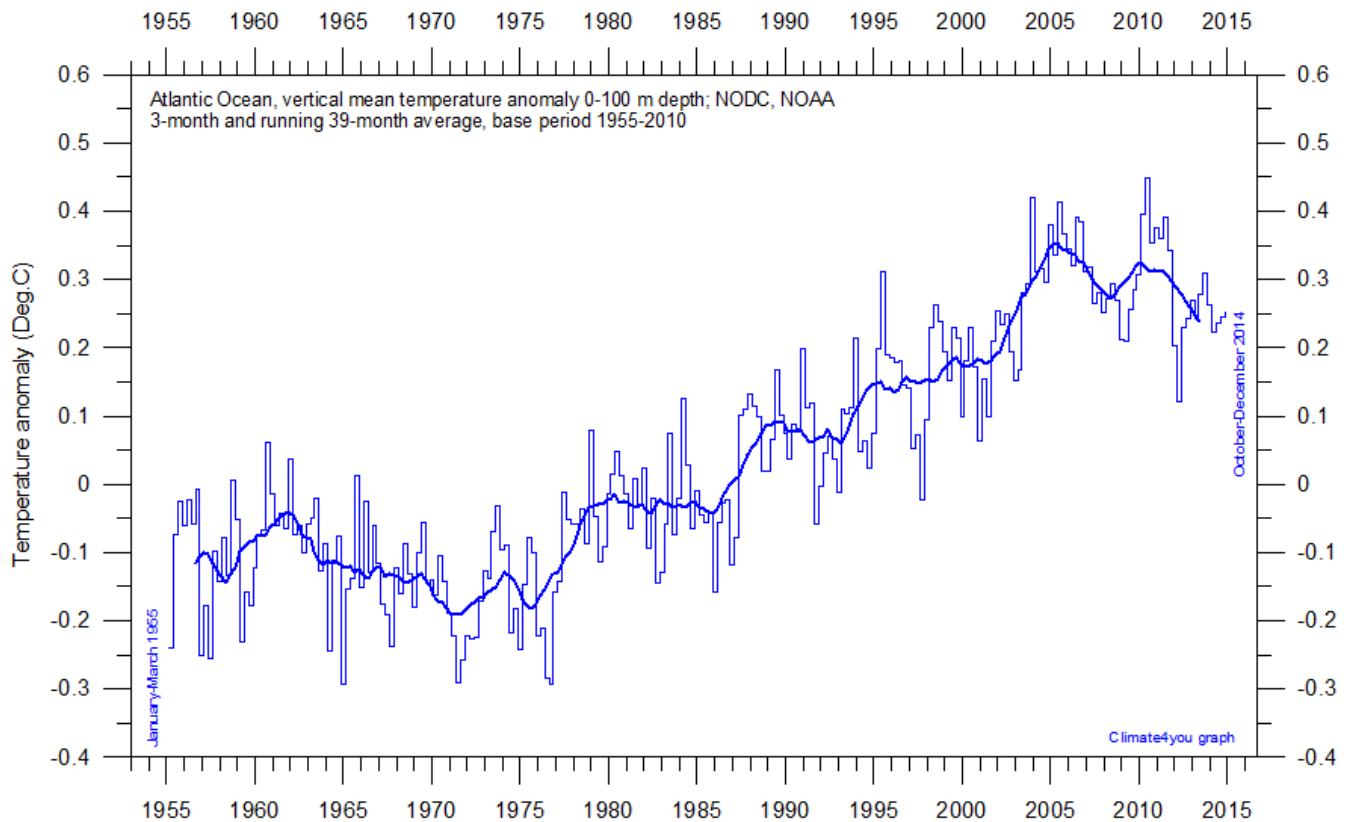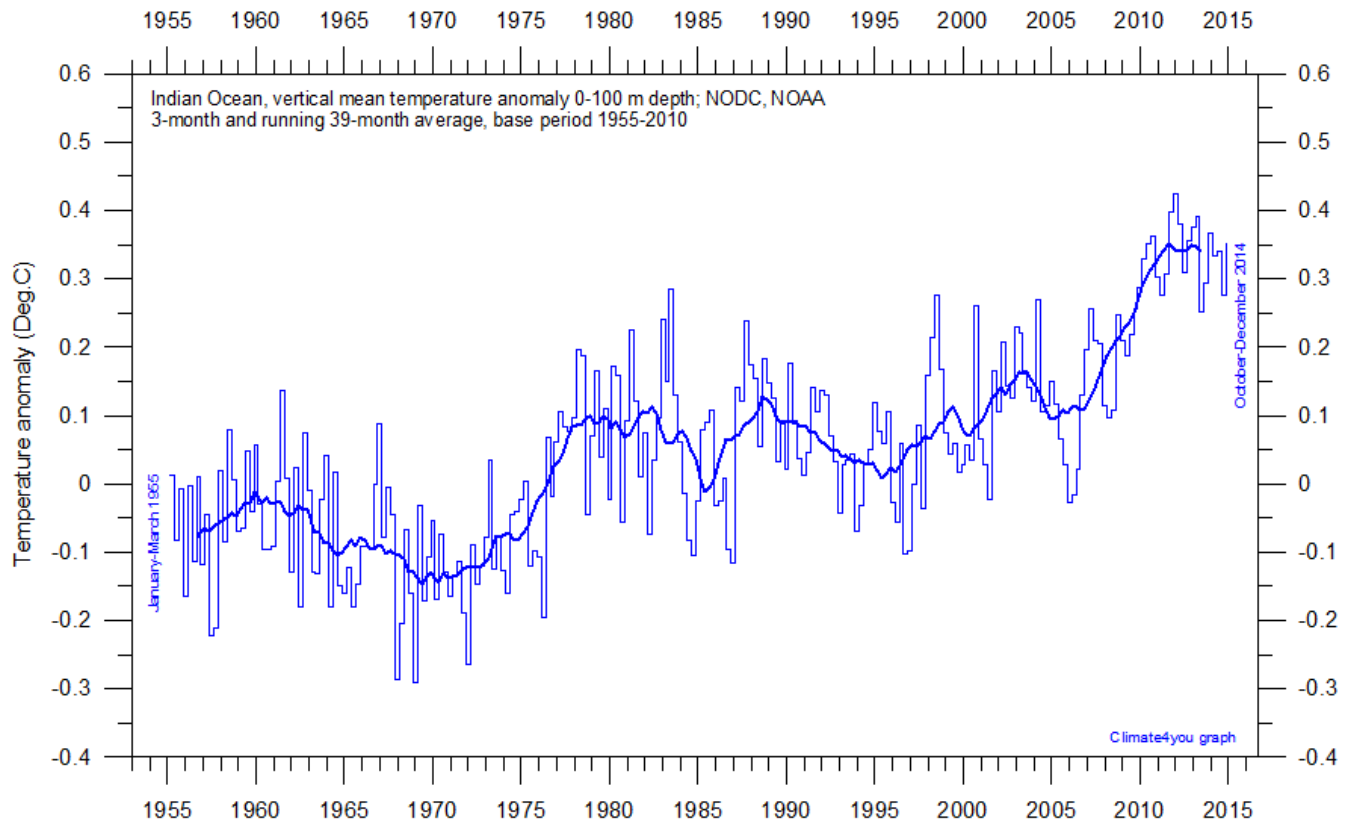
Indian Ocean vertical average temperature 0-100 m depth since 1955. The thin line indicate 3-month values, and the thick line represents the simple running 39-month (c. 3 year) average. Data source: NOAA National Oceanographic Data Center (NODC). Base period 1955-2010.

15

North Atlantic heat content uppermost 700 m, updated to December 2014
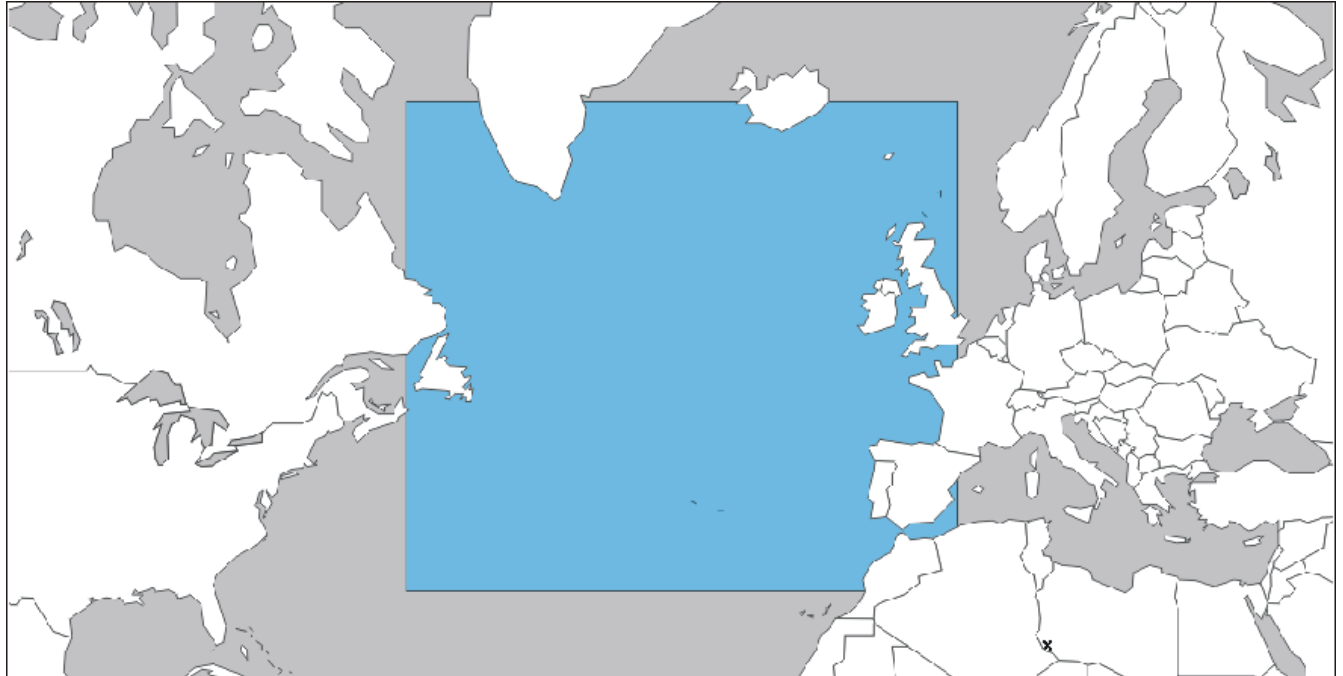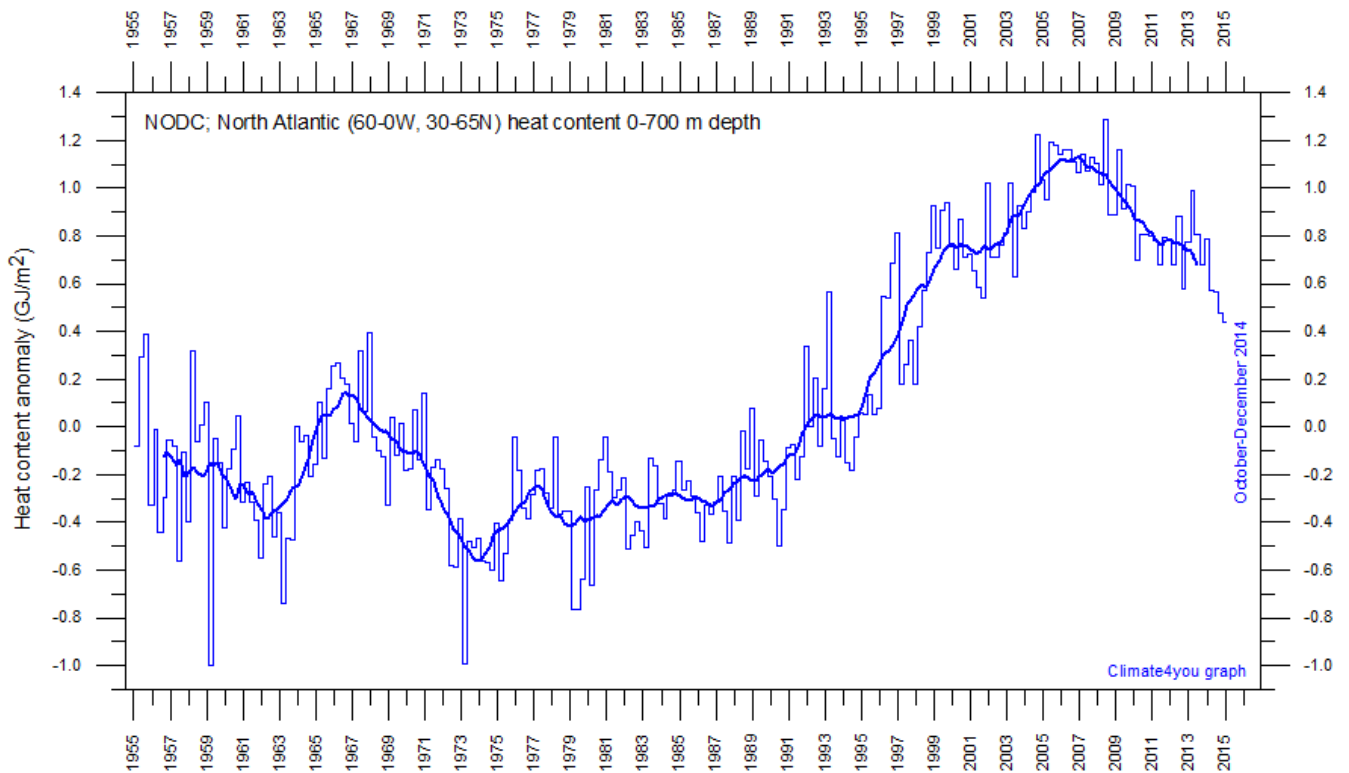
Global monthly heat content anomaly (GJ/m2) in the uppermost 700 m of the North Atlantic (60-0W, 30-65N; see map above) *ocean since January 1955. The thin line indicates monthly values, and the thick line represents the simple running 37 month (c. 3 year) average. Data source: National Oceanographic Data Center (NODC).*

Depth-temperature diagram along 59 N across the North Atlantic, extending from northern Labrador in the west to northern Scotland in the east, using Argo-data. The uppermost panel shows the temperature, and the lower diagram shows the temperature anomaly, using the monthly average temperature 2004-2013 as reference. Source: Global Marine Argo Atlas.

North Atlantic sea temperatures 30-0W at 59N, updated to October 2014
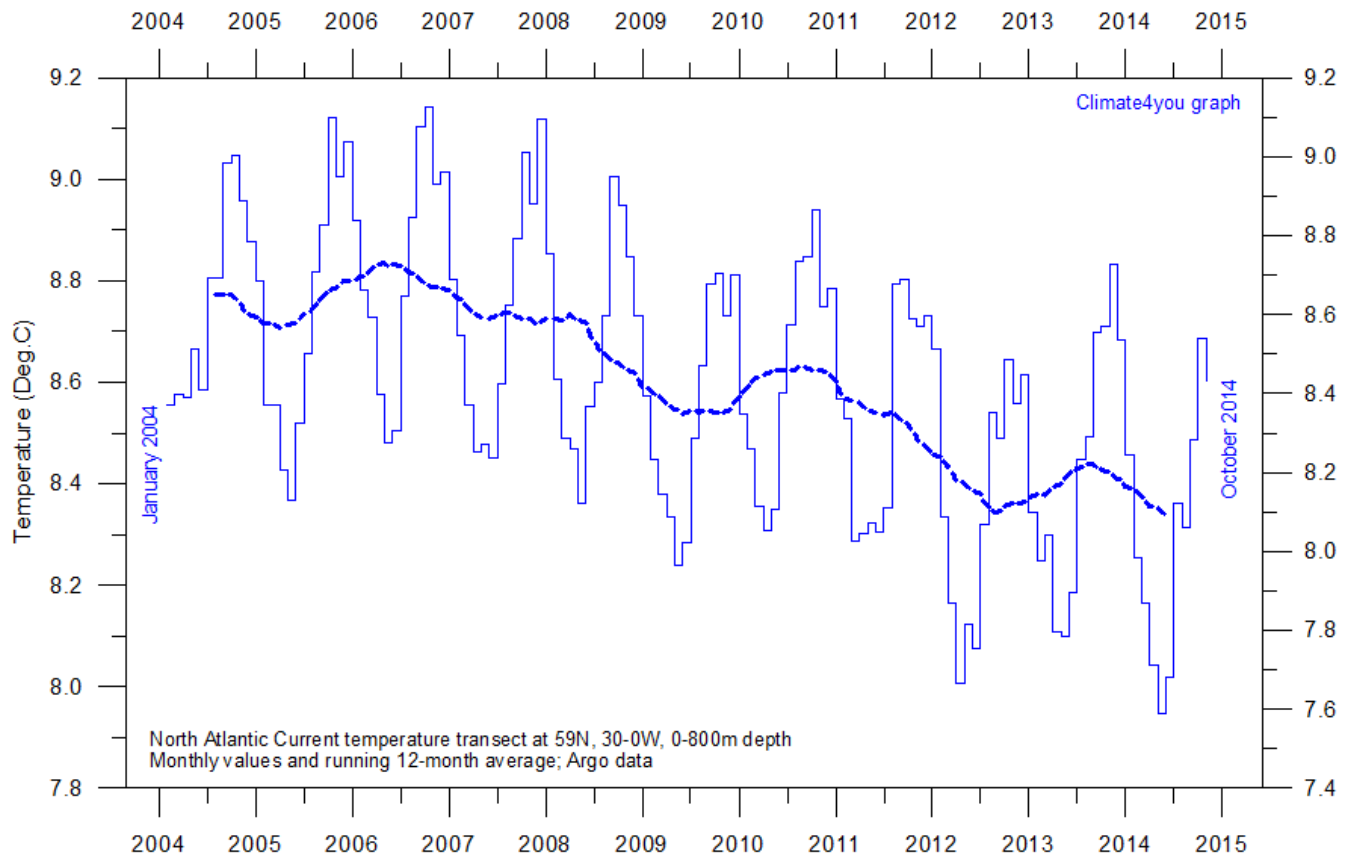
Average temperature along 59 N, 30-0W, 0-800m depth, corresponding to the main part of the North Atlantic Current, using Argo-data. Source: Global Marine Argo Atlas. Additional information can be found in: Roemmich, D. and J. Gilson, 2009. The 2004-2008 mean and annual cycle of temperature, salinity, and steric height in the global ocean from the Argo Program. Progress in Oceanography, 82, 81-100.

Troposphere and stratosphere temperatures from satellites, updated to January 2015
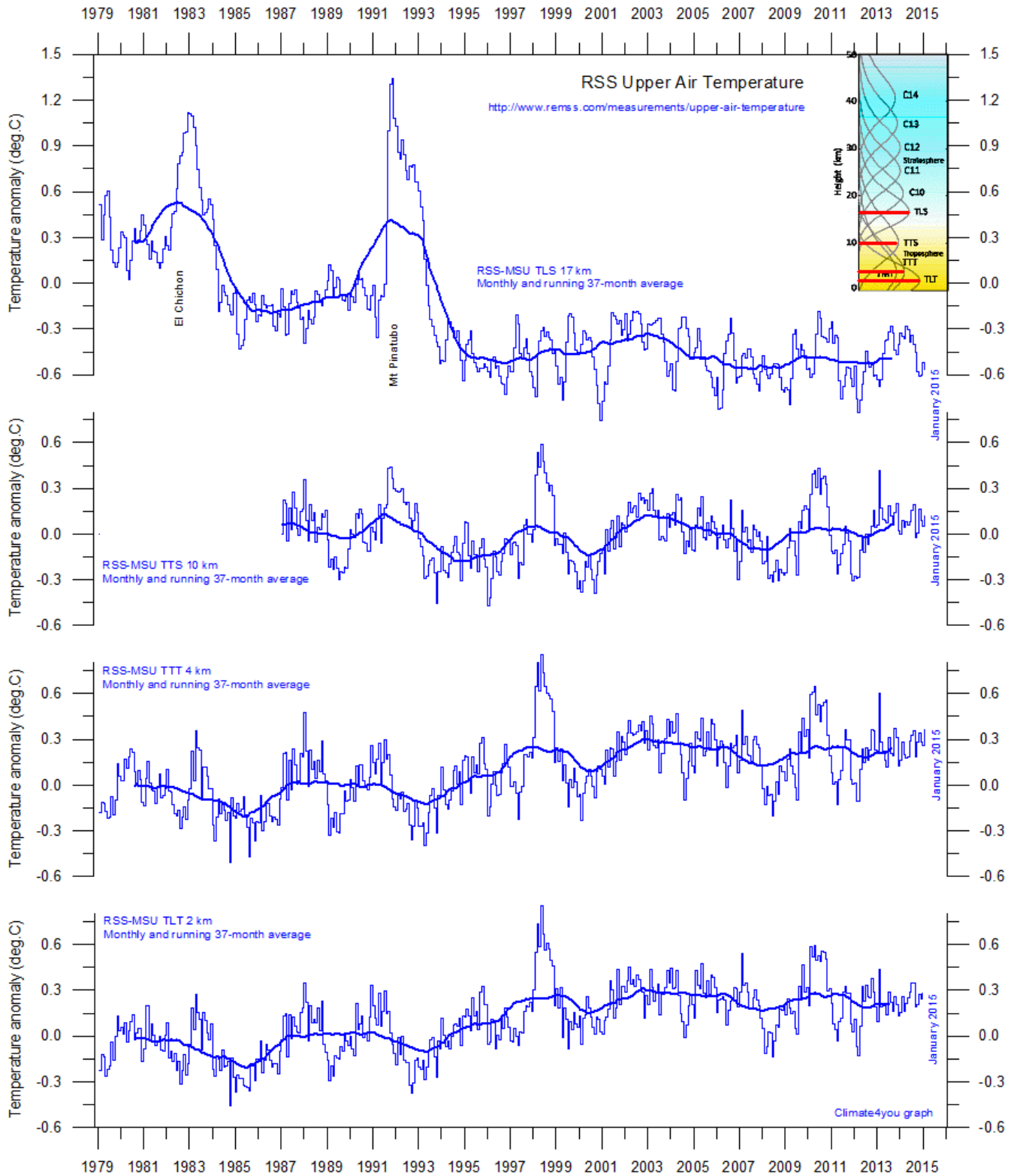
Global monthly average temperature in different altitudes according to Remote Sensing Systems (RSS). The thin lines represent the monthly average, and the thick line the simple running 37 month average, nearly corresponding to a running 3 yr average.

Zonal lower troposphere temperatures from satellites, updated to January 2015
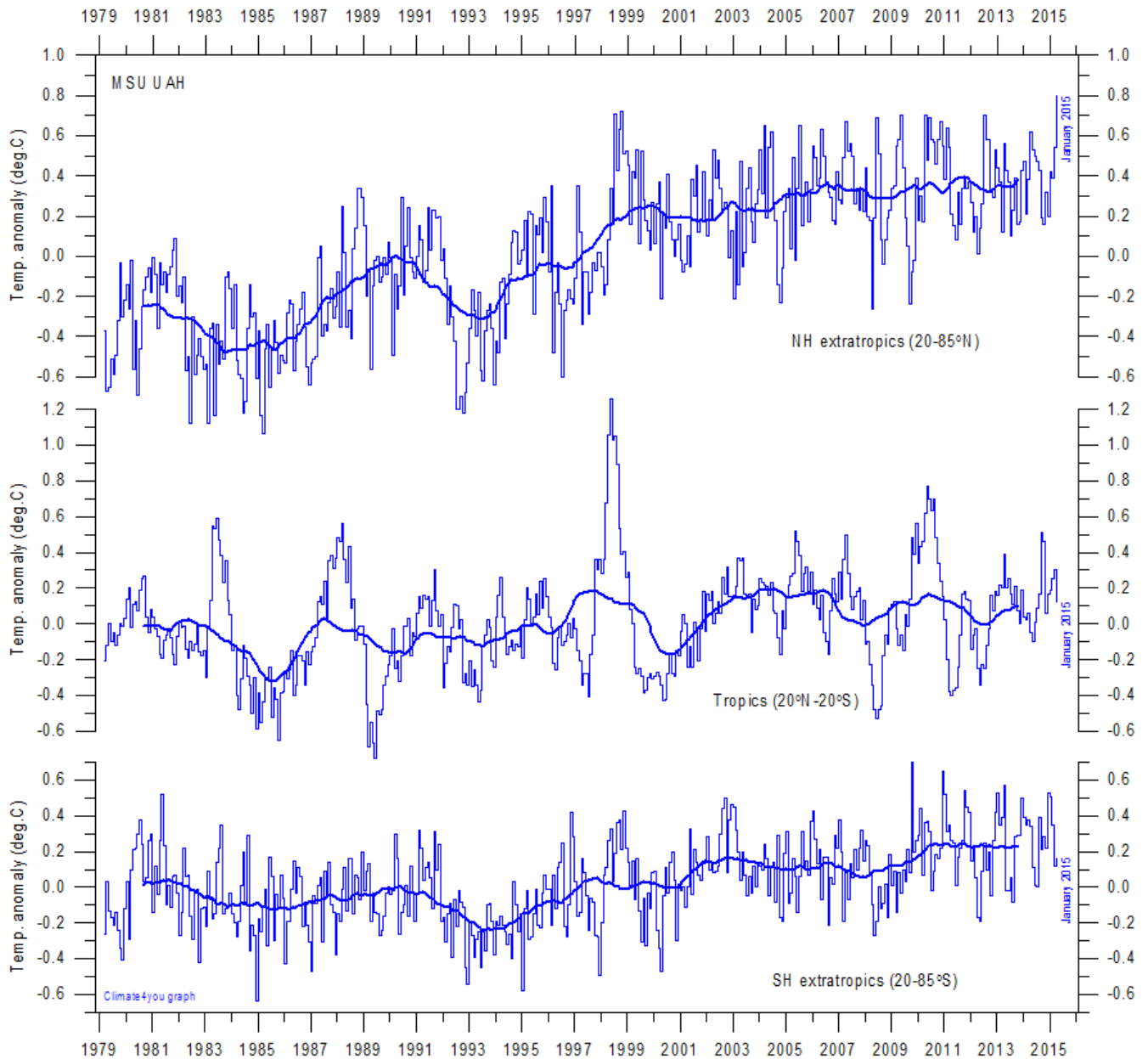
Global monthly average lower troposphere temperature since 1979 for the tropics and the northern and southern extratropics, according to [University of Alabama](#) at Huntsville, USA. Thin lines show the monthly temperature. Thick lines represent the simple running 37-month average, nearly corresponding to a running 3 yr average. Reference period 1981-2010.

Arctic and Antarctic lower troposphere temperature, updated to January 2015
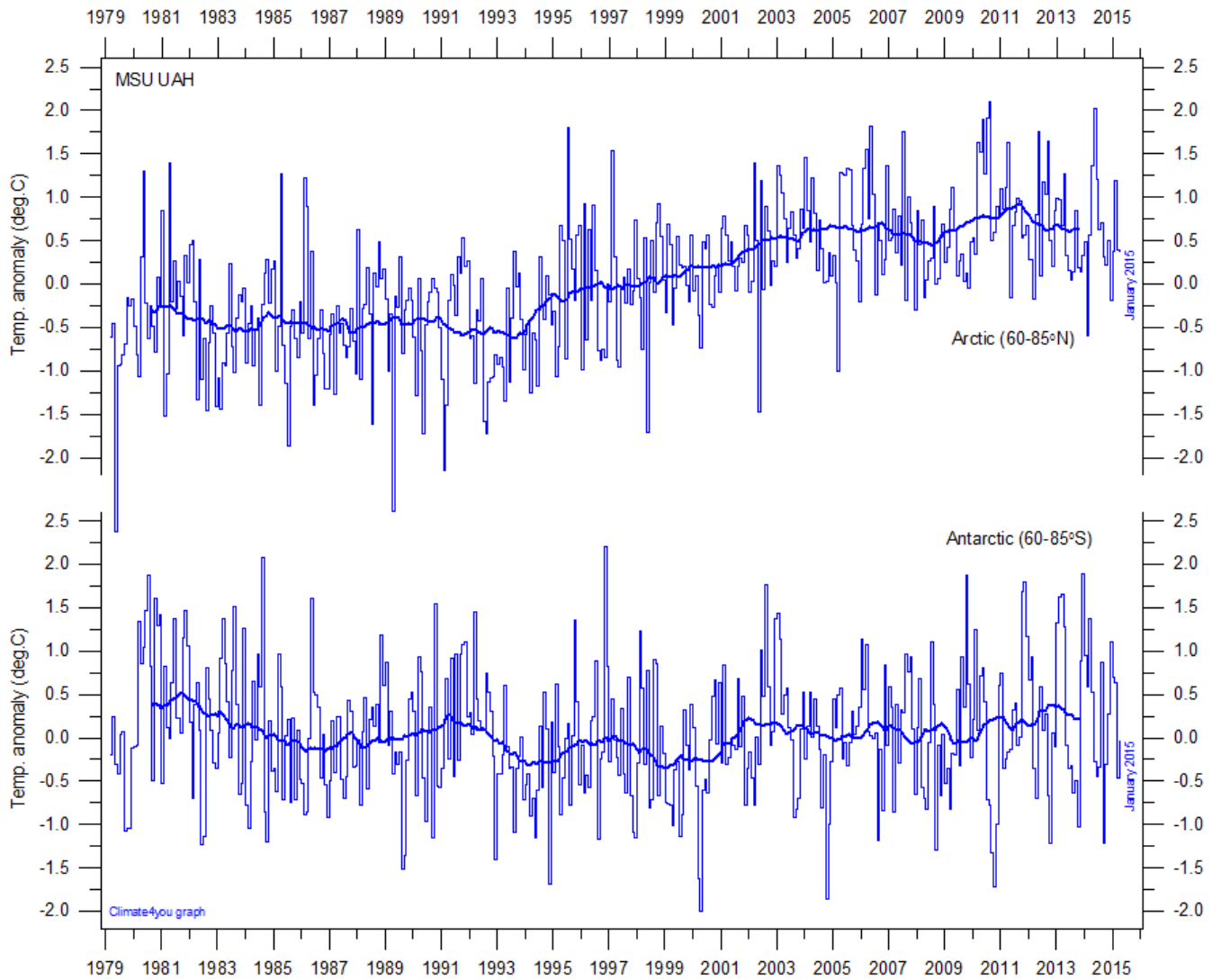
Global monthly average lower troposphere temperature since 1979 for the North Pole and South Pole regions, based on satellite observations (University of Alabama at Huntsville, USA). Thin lines show the monthly temperature. The thick line is the simple running 37-month average, nearly corresponding to a running 3 yr average.

Diagram showing area weighted Arctic (70-90°N) monthly surface air temperature anomalies (HadCRUT4) since January 2000, in relation to the WMO normal period 1961-1990. The thin blue line shows the monthly temperature anomaly, while the thicker red line shows the running 37 month (c.3 yr) average.

Diagram showing area weighted Antarctic (70-90°N) monthly surface air temperature anomalies (HadCRUT4) since January 2000, in relation to the WMO normal period 1961-1990. The thin blue line shows the monthly temperature anomaly, while the thicker red line shows the running 37 month (c.3 yr) average.

Diagram showing area weighted Arctic (70-90⁰N) monthly surface air temperature anomalies (HadCRUT4) since January 1957, in relation to the WMO normal period 1961-1990. The thin blue line shows the monthly temperature anomaly, while the thicker red line shows the running 37 month (c.3 yr) average.

Diagram showing area weighted Antarctic (70-90⁰N) monthly surface air temperature anomalies (HadCRUT4) since January 1957, in relation to the WMO normal period 1961-1990. The thin blue line shows the monthly temperature anomaly, while the thicker red line shows the running 37 month (c.3 yr) average.
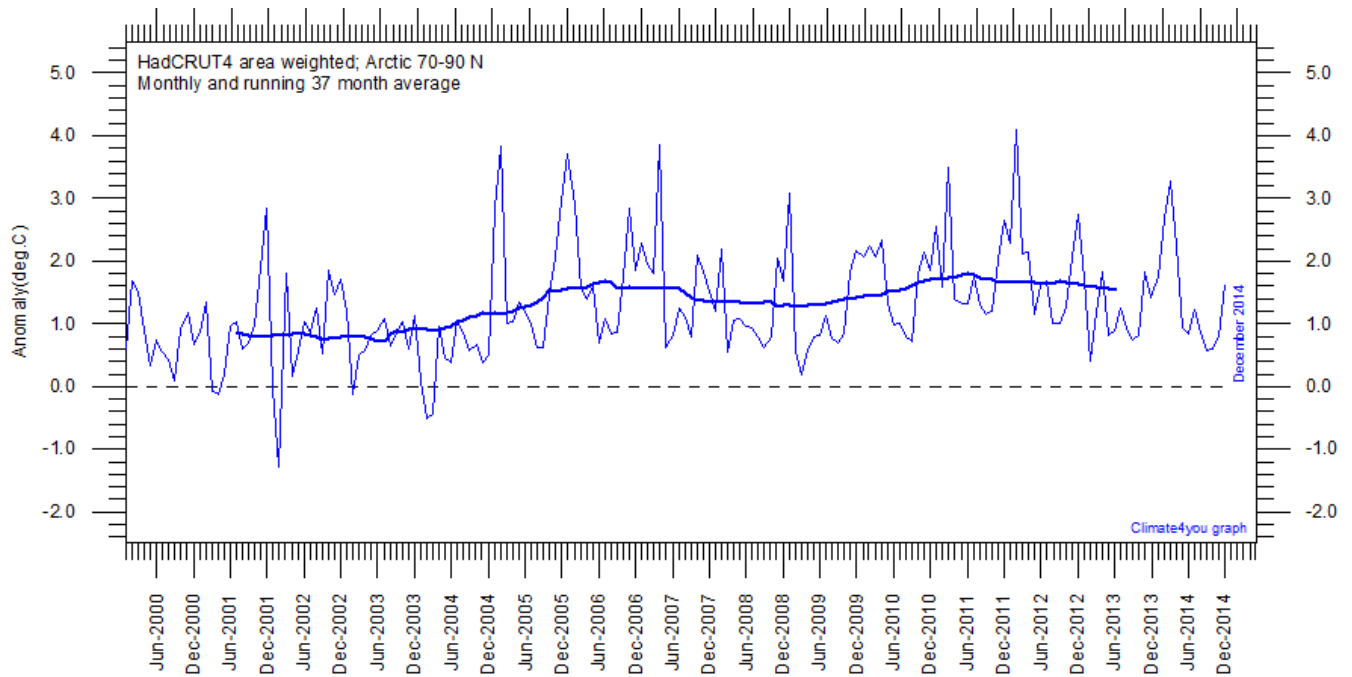
Diagram showing area-weighted Arctic (70-90°N) monthly surface air temperature anomalies (HadCRUT4) since January 1920, in relation to the WMO normal period 1961-1990. The thin blue line shows the monthly temperature anomaly, while the thi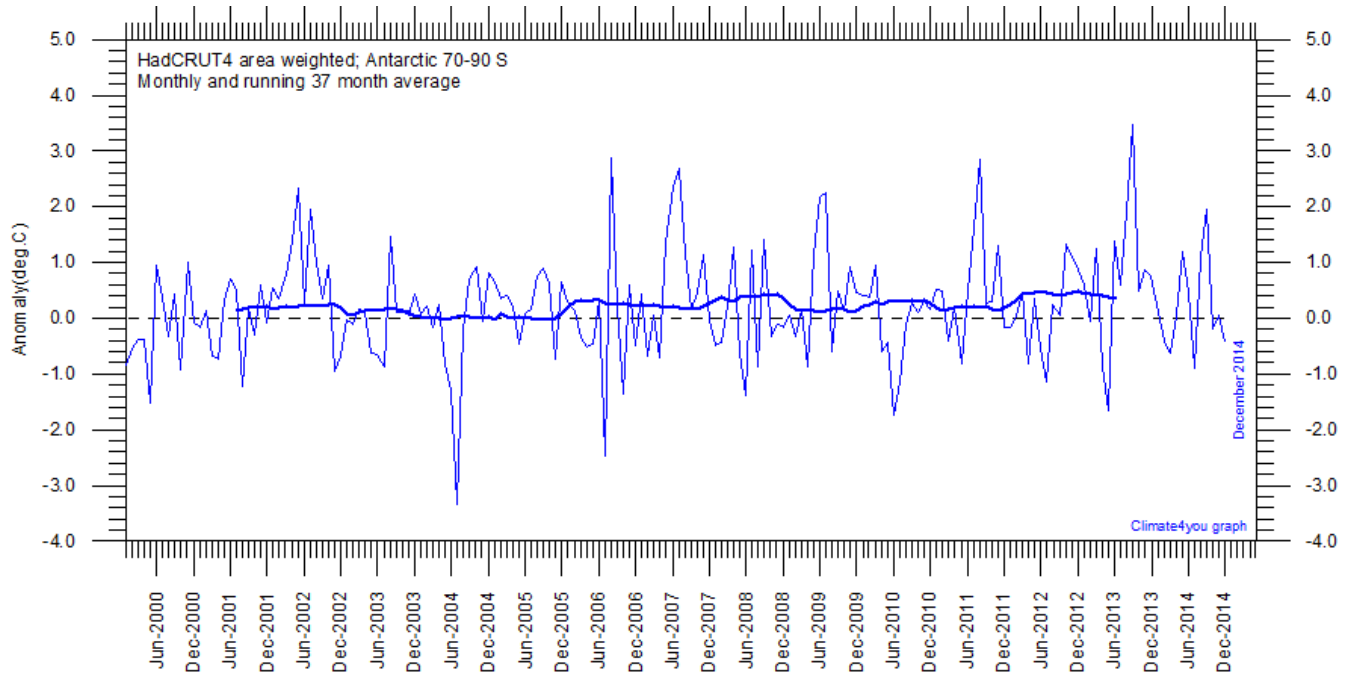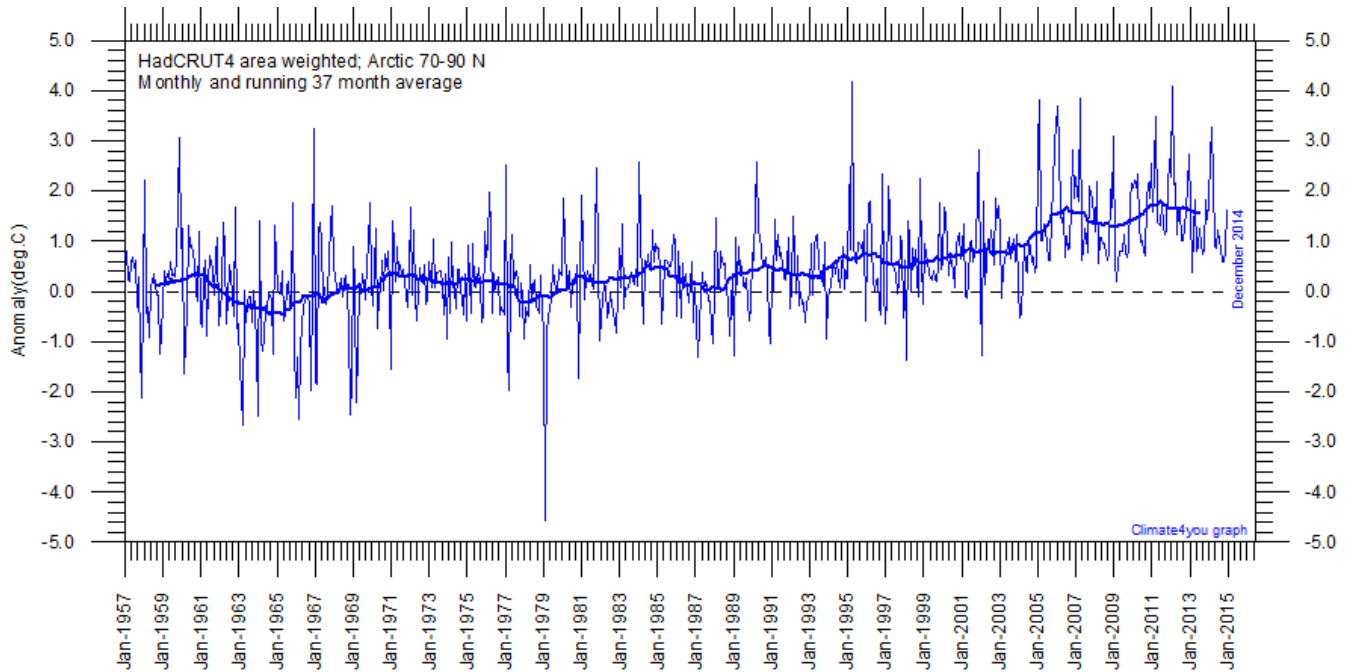cker red line shows the running 37 month (c.3 yr) average. Because of the relatively small number of Arctic stations before 1930, month-to-month variations in the early part of the temperature record are larger than later. The period from about 1930 saw the establishment of many new Arctic meteorological stations, first in Russia and Siberia, and following the 2nd World War, also in North America. The period since 2000 is warm, about as warm as the period 1930-1940.

24

As the HadCRUT4 data series has improved high latitude coverage data coverage (compared to the HadCRUT3 series) the individual 5°x5° grid cells has been weighted according to their surface area. This is in contrast to Gillet et al. 2008 which calculated a simple average, with no consideration to the surface area represented by the individual 5°x5° grid cells.

Literature:

Gillett, N.P., Stone, D.A., Stott, P.A., Nozawa, T., Karpechko, A.Y.U., Hegerl, G.C., Wehner, M.F. and Jones, P.D. 2008. Attribution of polar warming to human influence. *Nature Geoscience* 1, 750-754.

Arctic and Antarctic sea ice, updated to January 2015
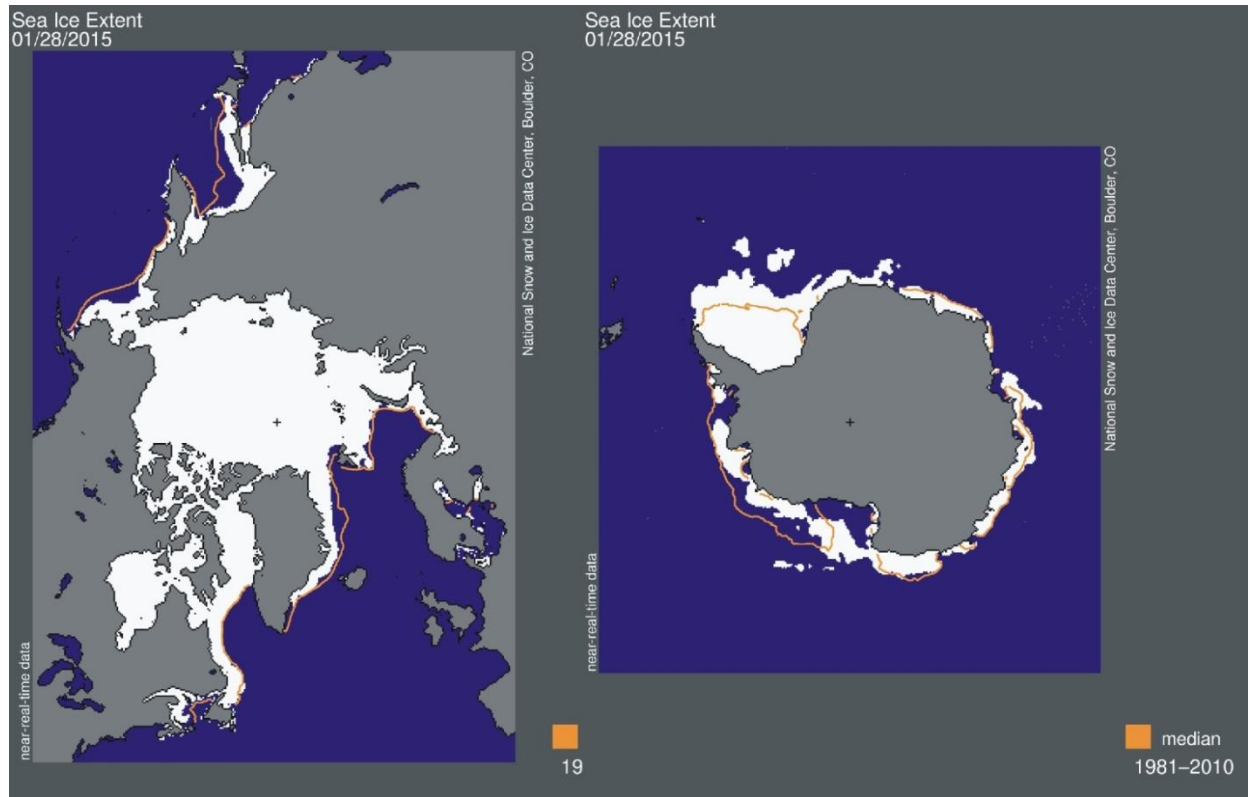
Sea ice extent 28 January 2015. The 'normal' or average limit of sea ice (orange line) is defined as 15% sea ice cover, according to the average of satellite observations 1981-2010 (both years inclusive). Sea ice may therefore well be encountered outside and open water areas inside the limit shown in the diagrams above. Map source: National Snow and Ice Data Center *(NSIDC).*
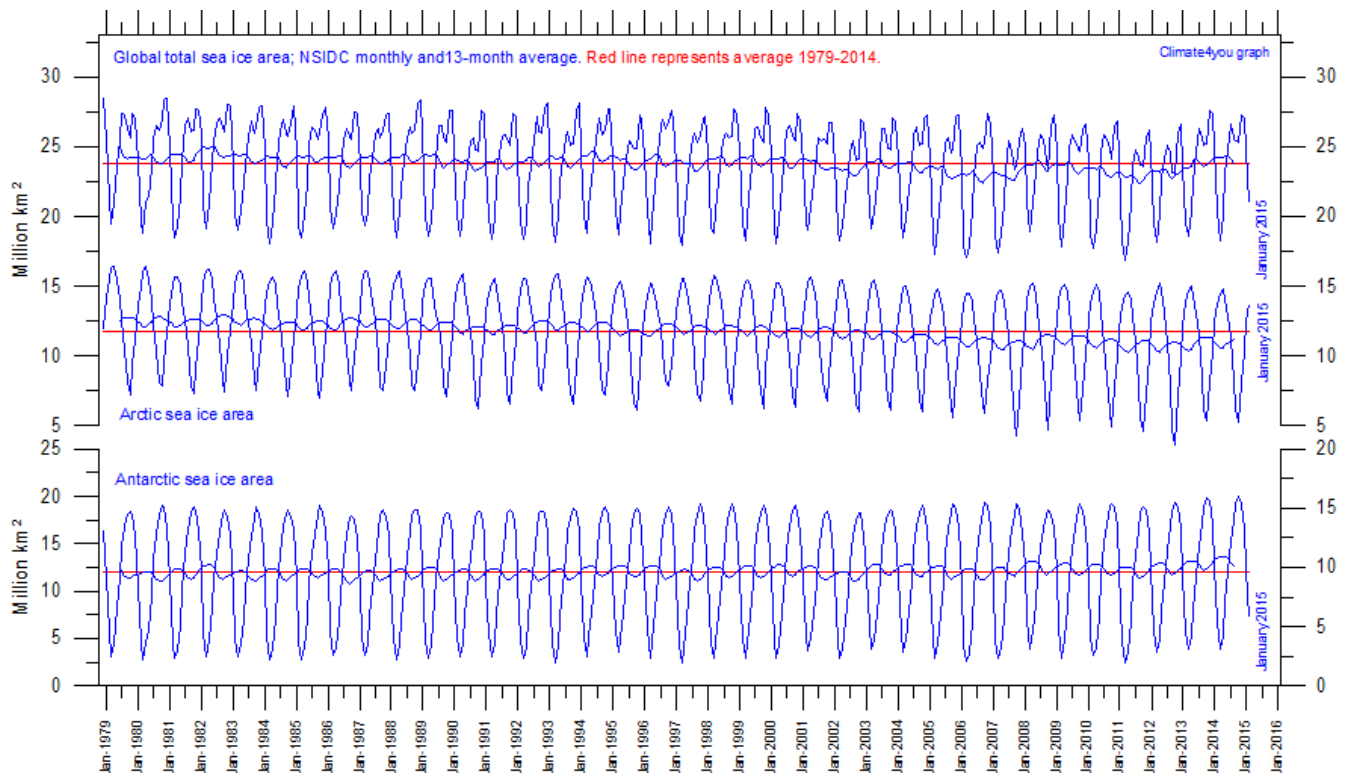
Graphs showing monthly Antarctic, Arctic and global sea ice extent since November 1978, according to the National Snow and Ice data Center (NSIDC).
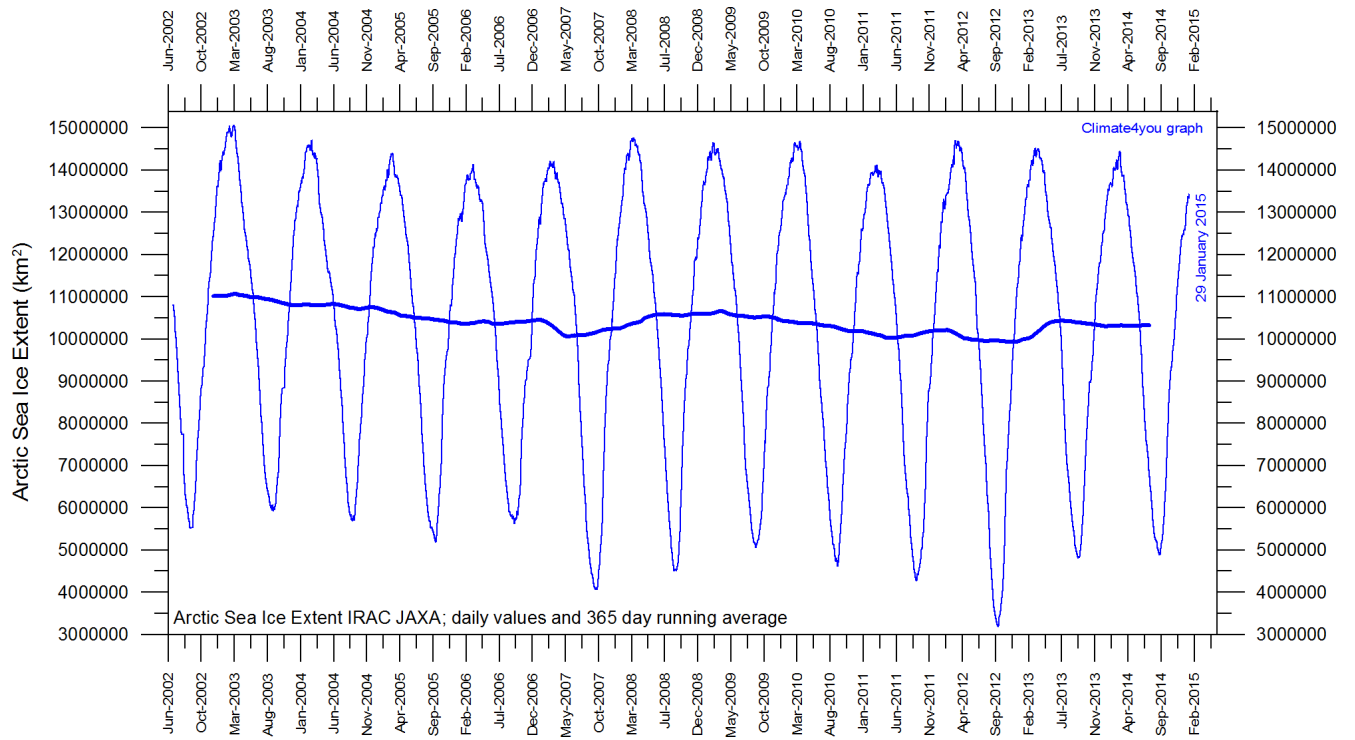
Graph showing daily Arctic sea ice extent since June 2002, to 29 January 2015, by courtesy of [Japan Aerospace Exploration Agency](#) (JAXA).

ARCc0.08-03.9 Ice Thickness (m): 20150130
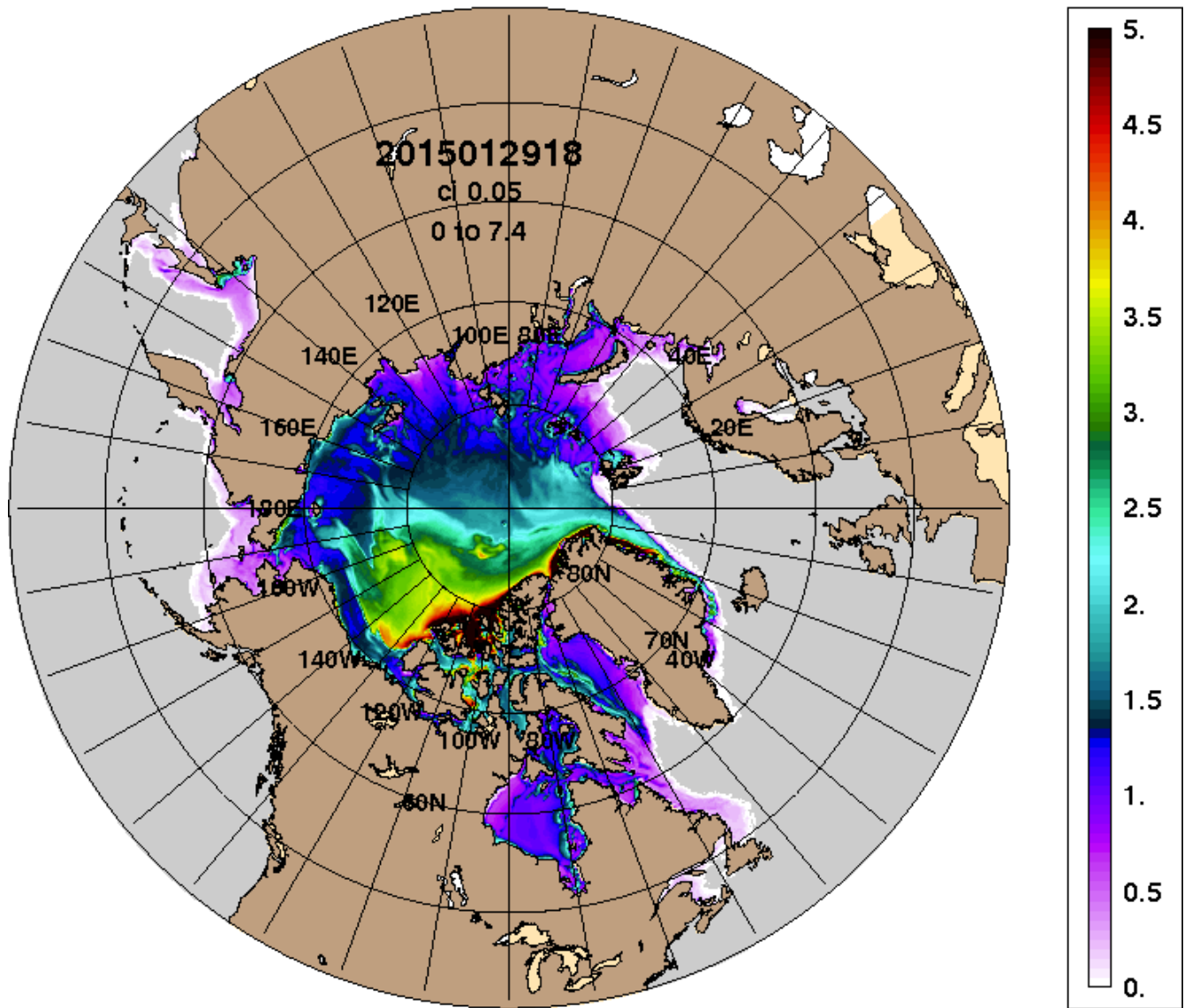
Northern hemisphere sea ice extension and thickness on 30 January 2015 according to the [Arctic Cap Nowcast/Forecast System](#) (ACNFS), US Naval Research Laboratory. Thickness scale (m) to the right.
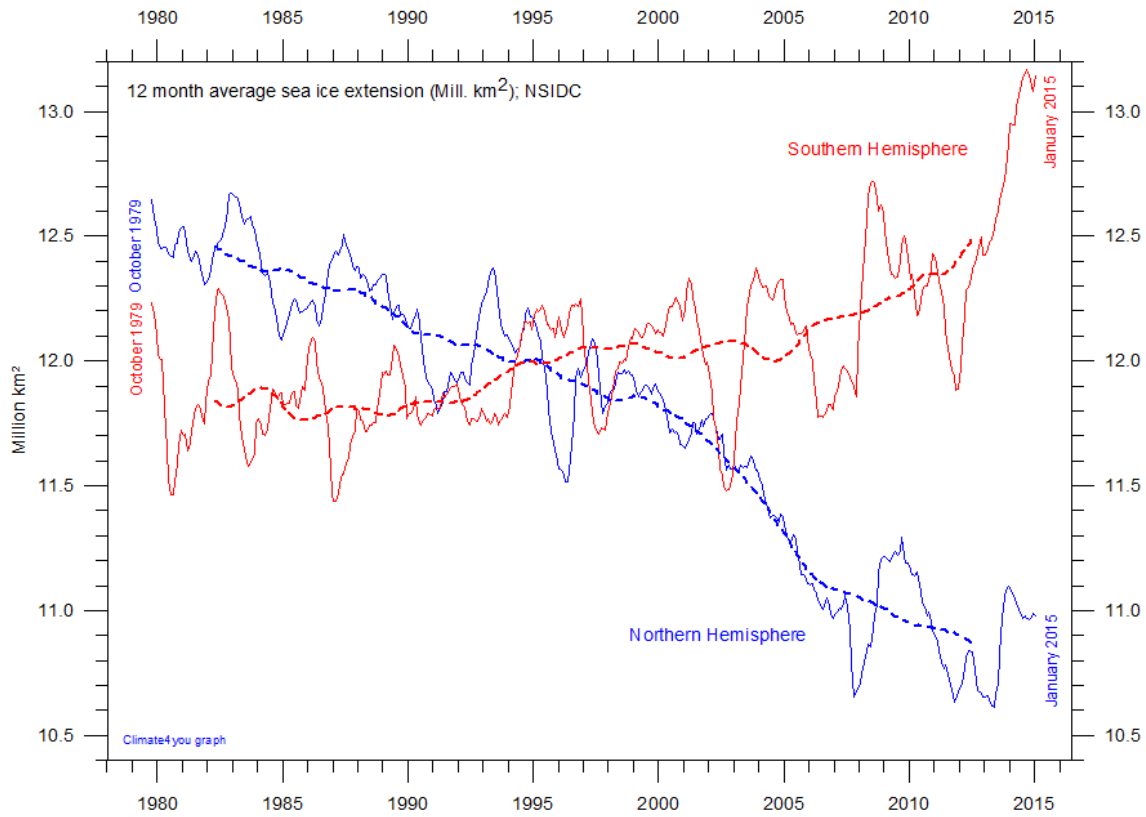
12 month running average sea ice extension in both hemispheres since 1979, the satellite-era. The October 1979 value represents the monthly average of November 1978 - October 1979, the November 1979 value represents the average of December 1978 - November 1979, etc. The stippled lines represent a 61-month (ca.5 years) average. Data source: National Snow and Ice Data Center (NSIDC).
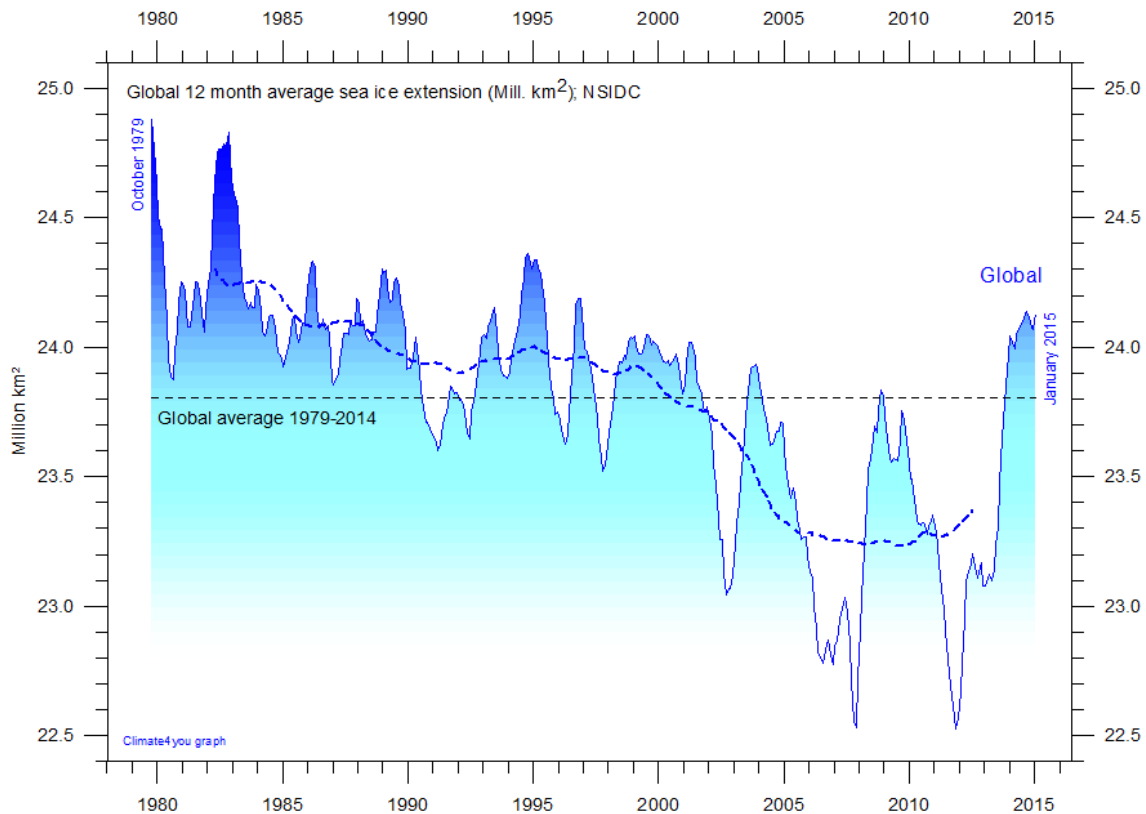
Global 12 month running average sea ice extension since 1979, the satellite-era. The October 1979 value represents the monthly average of November 1978 - October 1979, the November 1979 value represents the average of December 1978 - November 1979, etc. The stippled line represents a 61-month (ca.5 years) average. Data source: National Snow and Ice Data Center (NSIDC).

Global sea level, updated to August 2014
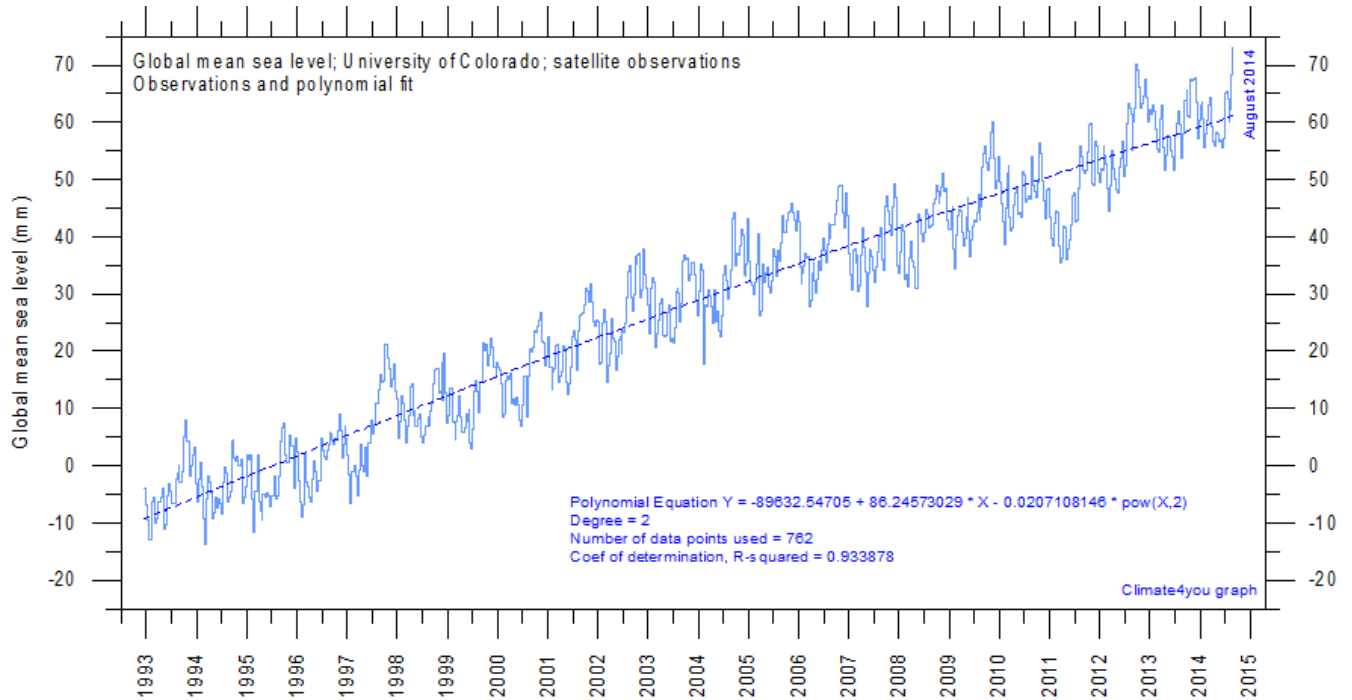
Global sea level (thin line) since late 1992 according to the Colorado Center for Astrodynamics Research at University of Colorado at Boulder. The thick stippled line represents a two-degree polynomium. The polynomium suggests the rate of the ongoing global sea level rise to be slowly decreasing. Time is shown along the x-axis as fractions of calendar years.
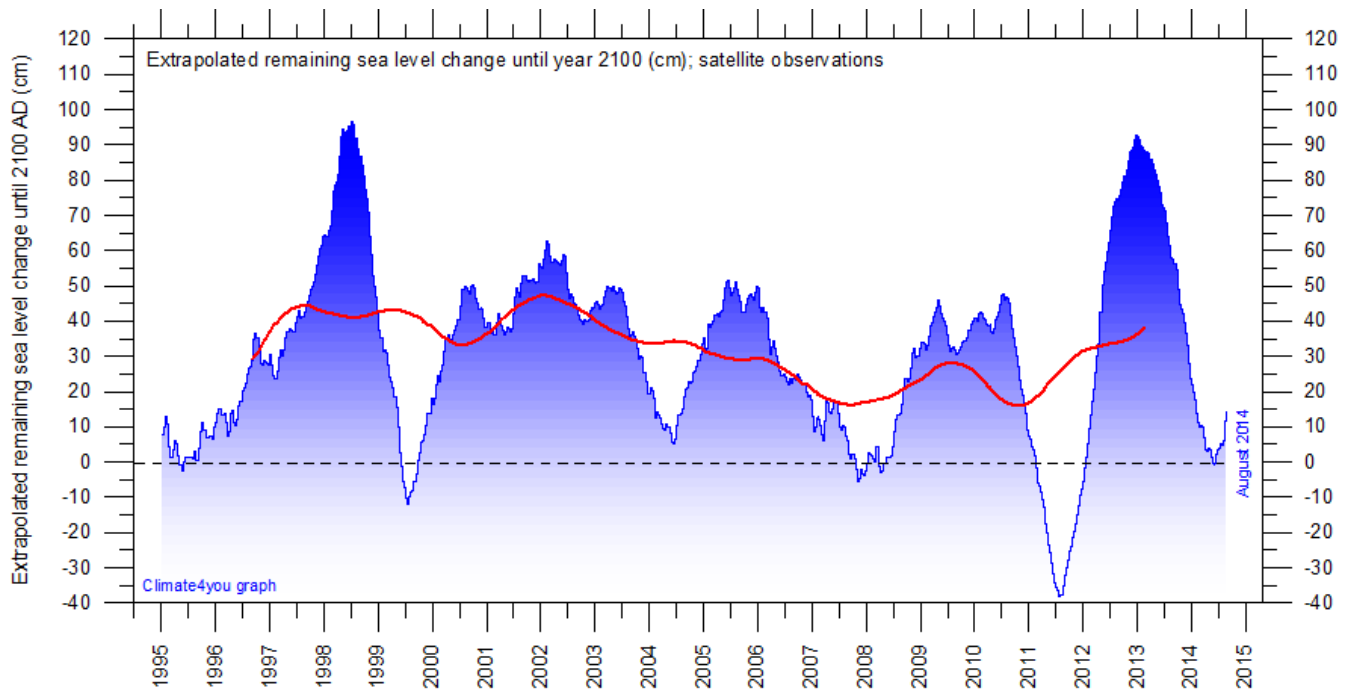
Forecasted change of global sea level until year 2100, based on simple extrapolation of measurements done by the Colorado Center for Astrodynamics Research at University of Colorado at Boulder, USA. The thick line is the simple running 3 yr average forecast for sea level change until year 2100. Based on this (thick line), the present simple empirical forecast of sea level change until 2100 is about +38 cm.

Northern Hemisphere weekly snow cover, updated to early January 2015
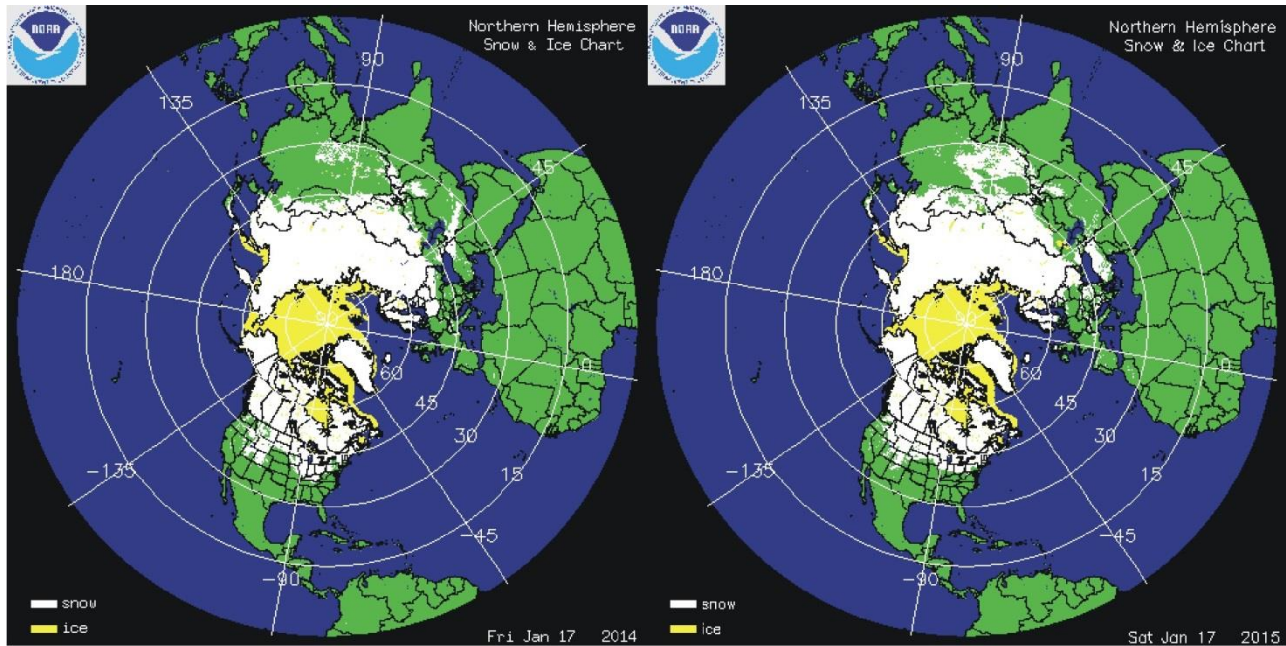
Northern hemisphere snow cover (white) and sea ice (yellow) 17 January 2014 (left) and 2015 (right). Map source: National Ice Center (NIC).
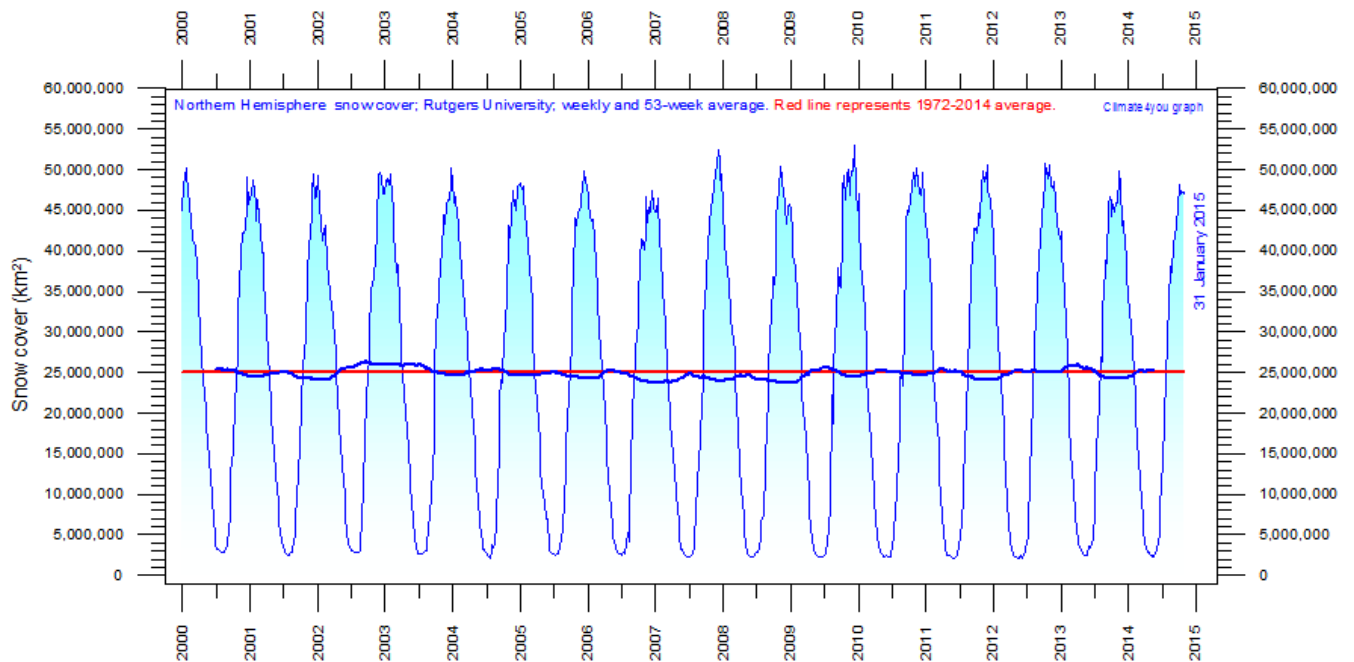
Northern hemisphere weekly snow cover since January 2000 according to Rutgers University Global Snow Laboratory. The thin blue line is the weekly data, and the thick blue line is the running 53-week average (approximately 1 year). The horizontal red line is the 1972-2014 average.
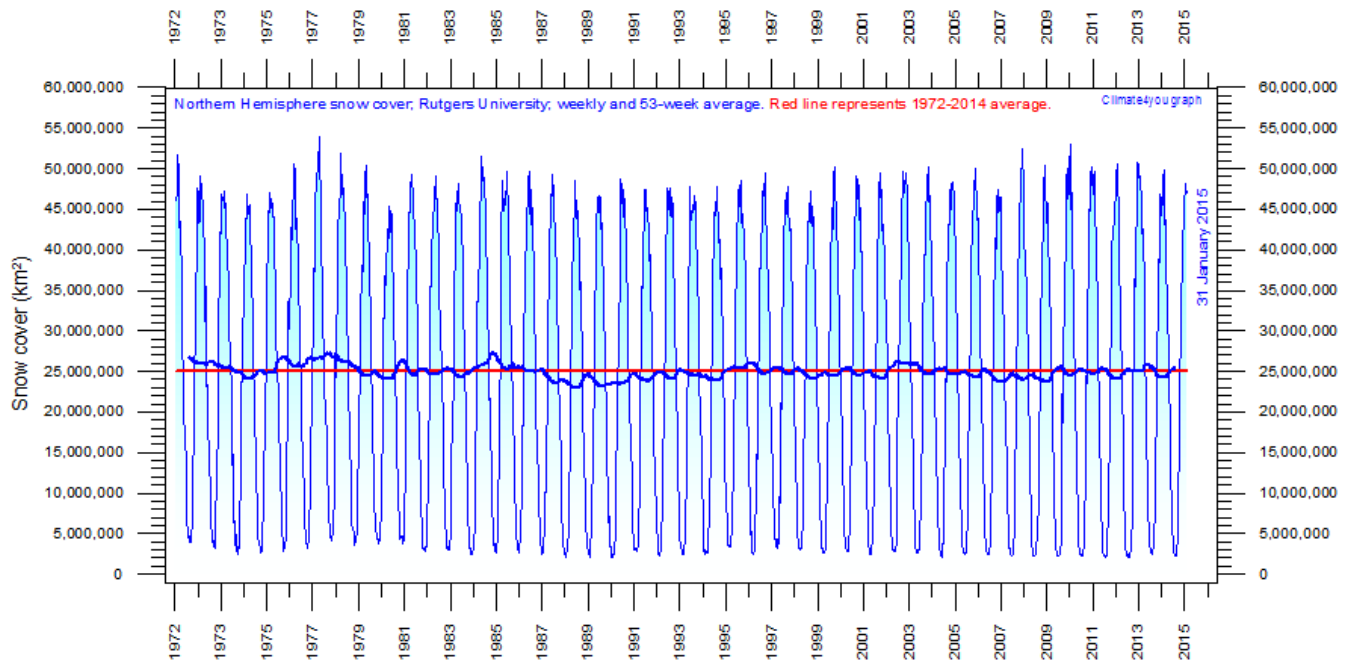
Northern hemisphere weekly snow cover since January 1972 according to Rutgers University Global Snow Laboratory. The thin blue line is the weekly data, and the thick blue line is the running 53-week average (approximately 1 year). The horizontal red line is the 1972-2014 average.

Atmospheric specific humidity, updated to January 2015
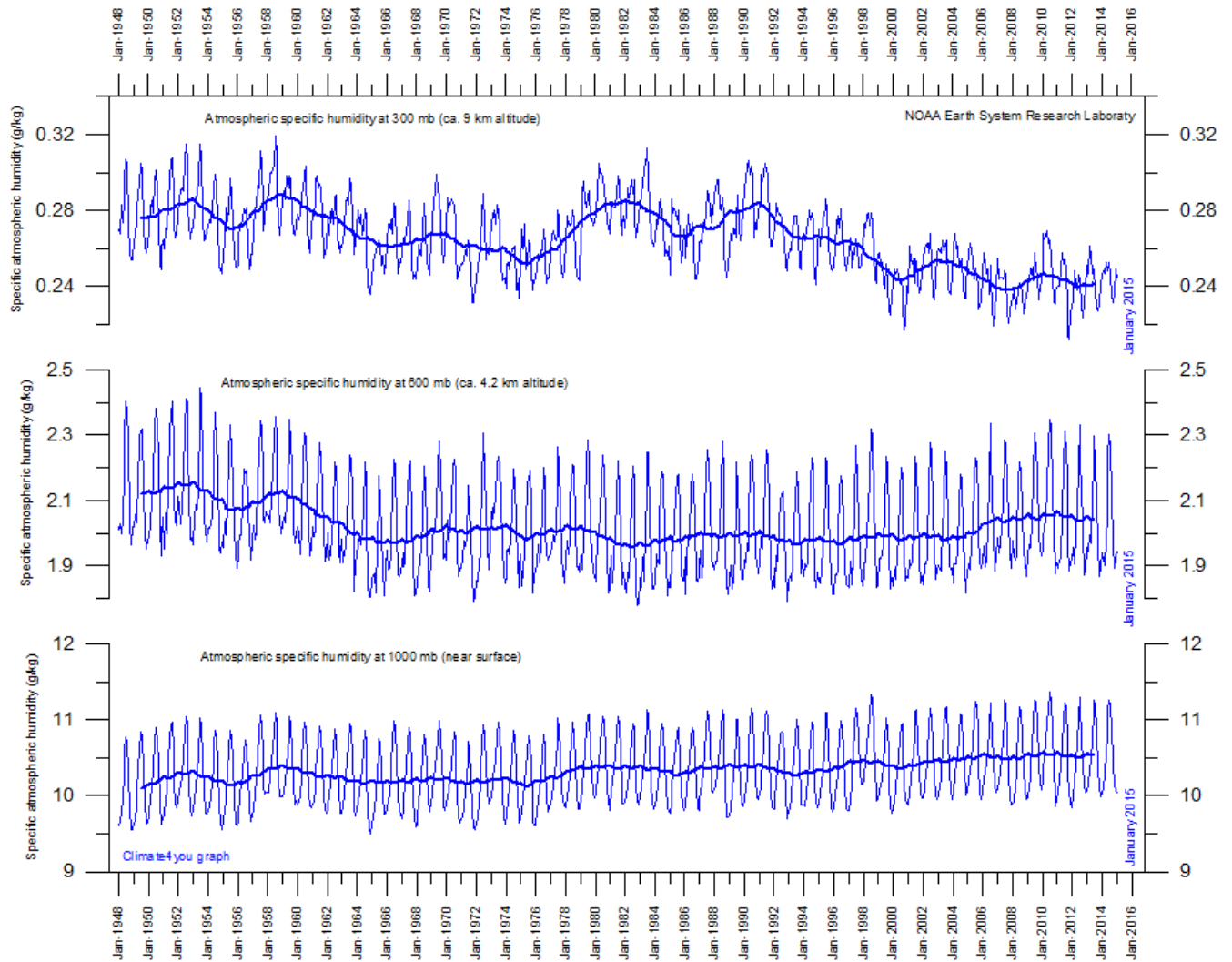
Specific atmospheric humidity (g/kg) at three different altitudes in the lower part of the atmosphere (*the Troposphere*) since January 1948 (*Kalnay et al. 1996*). The thin blue lines shows monthly values, while the thick blue lines show the running 37-month average (about 3 years). Data source: *Earth System Research Laboratory (NOAA)*.

Atmospheric CO₂, updated to January 2015
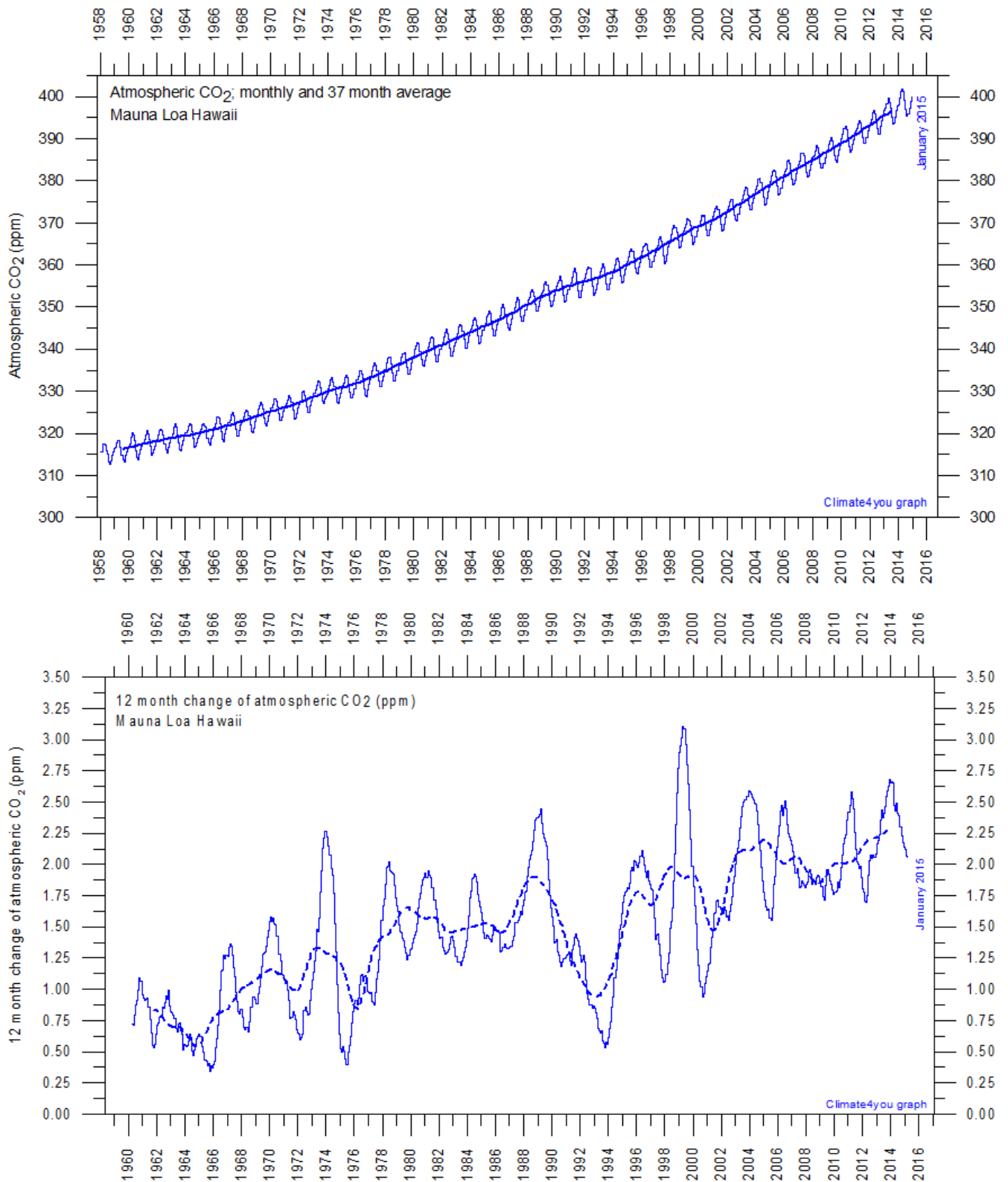
Monthly amount of atmospheric CO₂ (upper diagram) and annual growth rate (lower diagram); average last 12 months minus average preceding 12 months, thin line) of atmospheric CO₂ since 1959, according to data provided by the Mauna Loa Observatory, Hawaii, USA. The thick, stippled line is the simple running 37-observation average, nearly corresponding to a running 3 yr average.

The phase relation between atmospheric CO$_2$ and global temperature, updated to December 2014
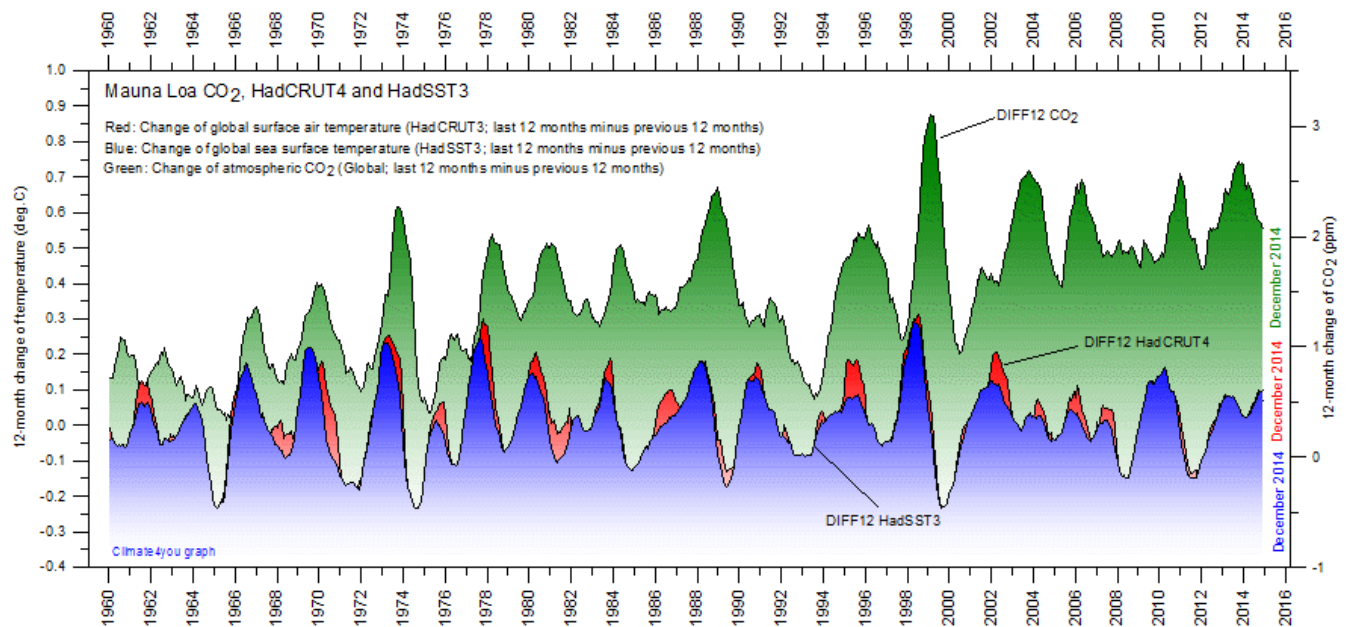
12-month change of global atmospheric CO$_2$ concentration (Mauna Loa; green), global sea surface temperature (HadSST3; blue) and global surface air temperature (HadCRUT4; red dotted). All graphs are showing monthly values of DIFF12, the difference between the average of the last 12 month and the average for the previous 12 months for each data series.

References:

Humlum, O., Stordahl, K. and Solheim, J-E. 2012. The phase relation between atmospheric carbon dioxide and global temperature. Global and Planetary Change, August 30, 2012.
http://www.sciencedirect.com/science/article/pii/S0921818112001658?v=s5
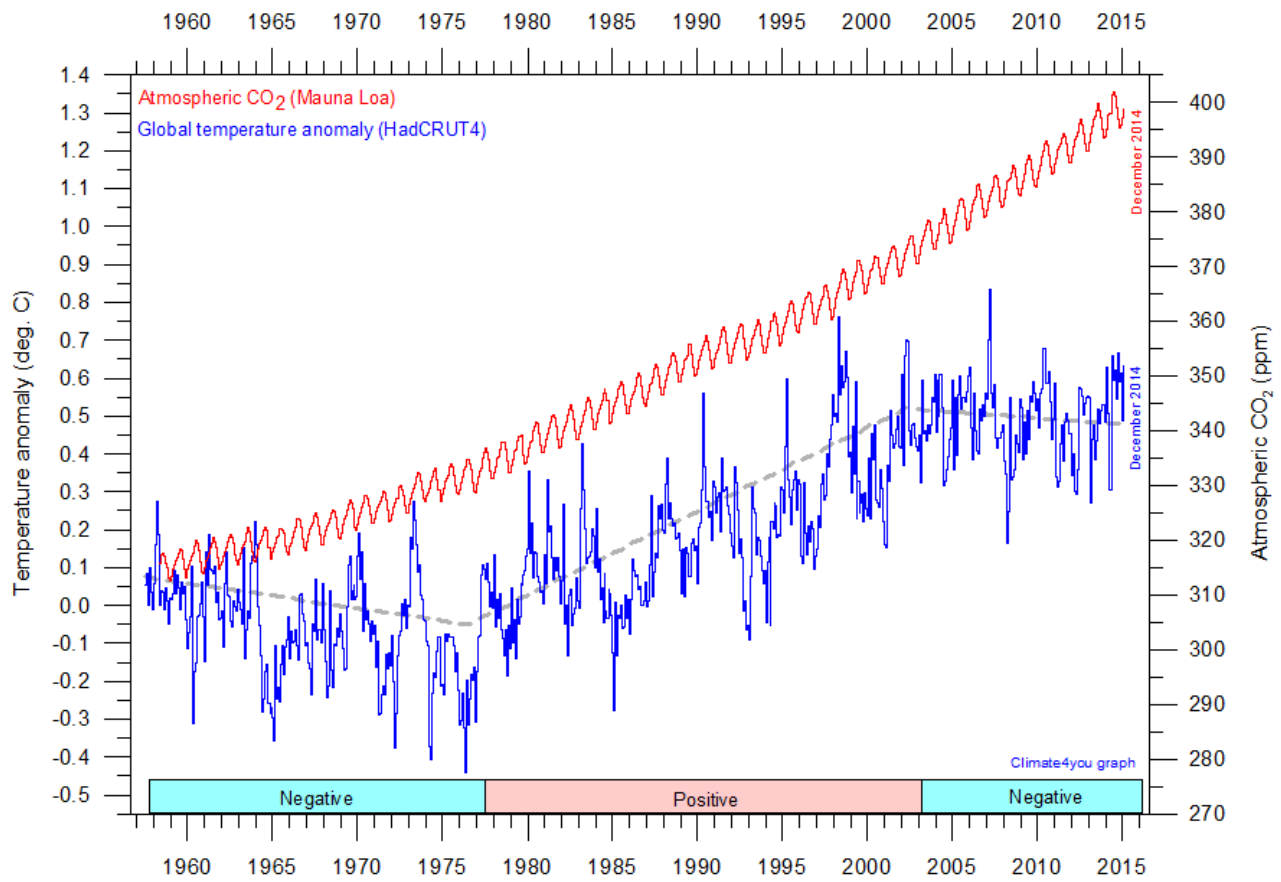
Global surface air temperature and atmospheric CO₂, updated to January 2015
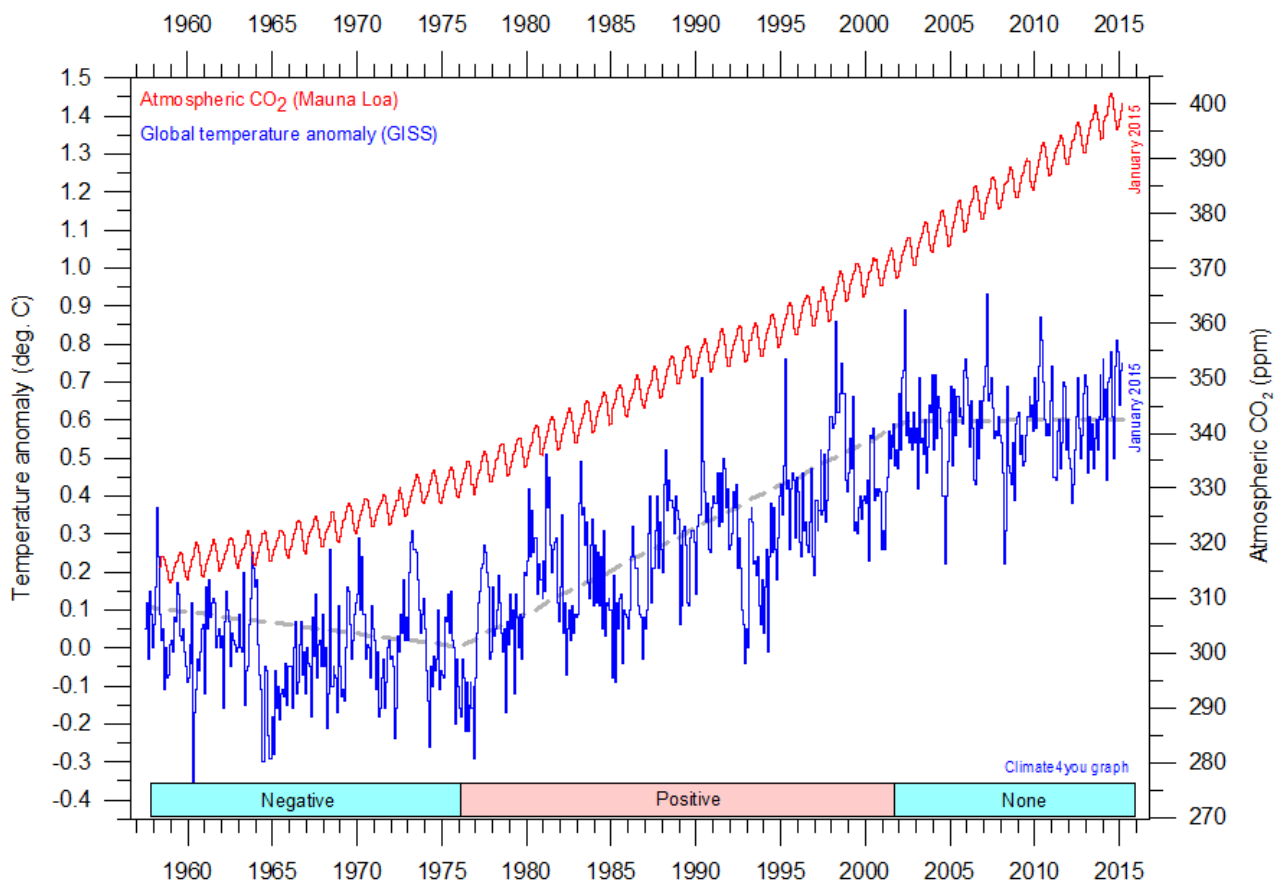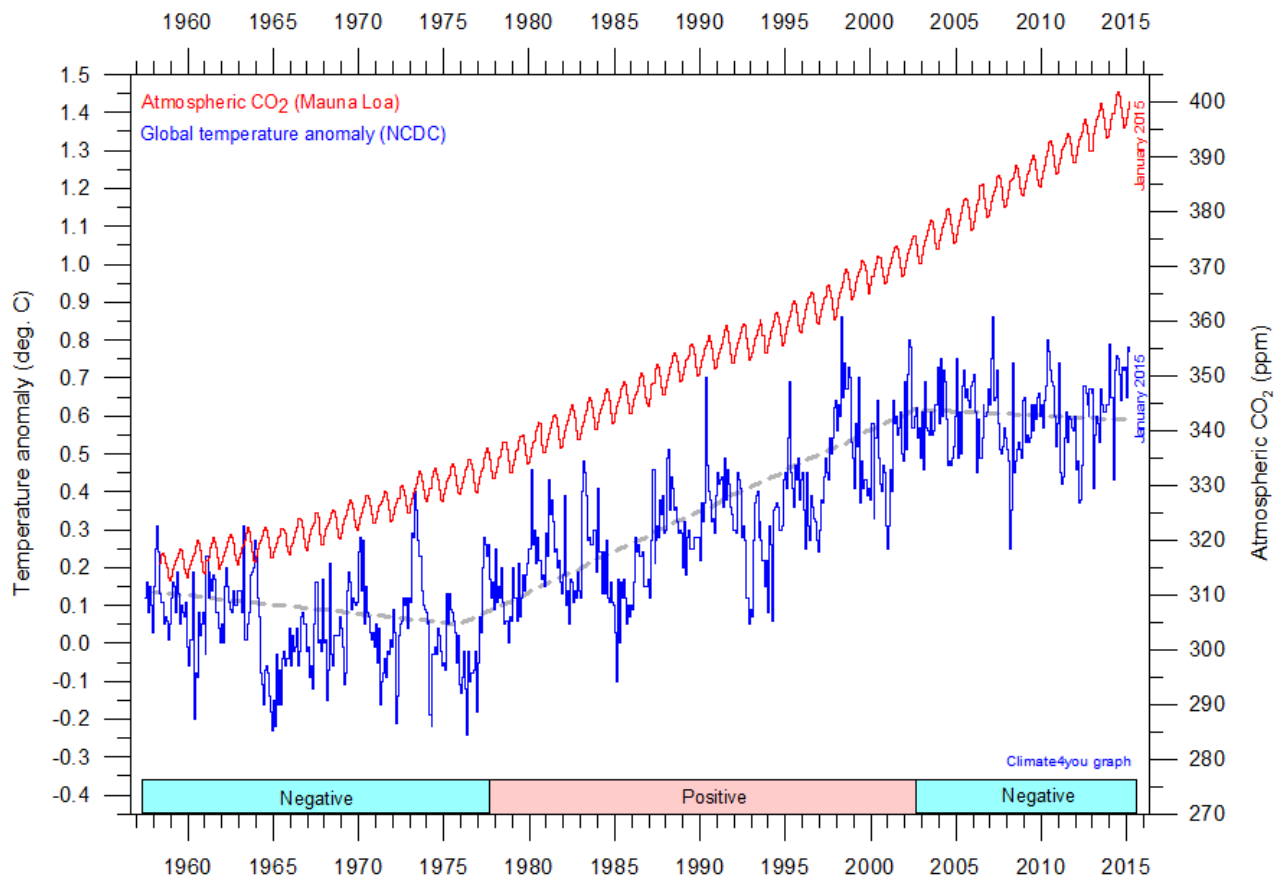
Diagrams showing HadCRUT3, GISS, and NCDC monthly global surface air temperature estimates (blue) and the monthly atmospheric CO_2 content (red) according to the [Mauna Loa Observatory](), Hawaii. The Mauna Loa data series begins in March 1958, and 1958 was therefore chosen as starting year for the diagrams. Reconstructions of past atmospheric CO_2 concentrations (before 1958) are not incorporated in this diagram, as such past CO_2 values are derived by other means (ice cores, stomata, or older measurements using different methodology), and therefore are not directly comparable with direct atmospheric measurements. The dotted grey line indicates the approximate linear temperature trend, and the boxes in the lower part of the diagram indicate the relation between atmospheric CO_2 and global surface air temperature, negative or positive. Please note that the HadCRUT4 diagram is not yet updated beyond December 2014.

Most climate models assume the greenhouse gas carbon dioxide CO_2 to influence significantly upon global temperature. It is therefore relevant to compare different temperature records with measurements of atmospheric CO_2, as shown in the diagrams above. Any comparison, however, should not be made on a monthly or annual basis, but for a longer time period, as other effects (oceanographic, etc.) may well override the potential influence of CO_2 on short time scales such as just a few years. It is of cause equally inappropriate to present new meteorological record values, whether daily, monthly or annual, as support for the hypothesis ascribing high importance of atmospheric CO_2 for global temperatures. Any such meteorological record value may well be the result of other phenomena.

What exactly defines the critical length of a relevant time period to consider for evaluating the alleged importance of CO_2 remains elusive, and is still a topic for discussion. However, the critical period length must be inversely proportional to the temperature sensitivity of CO_2, including feedback effects. If the net temperature effect of atmospheric CO_2 is strong, the critical time period will be short, and vice versa.

However, past climate research history provides some clues as to what has traditionally been considered the relevant length of period over

which to compare temperature and atmospheric CO_2. After about 10 years of concurrent global temperature- and CO_2-increase, IPCC was established in 1988. For obtaining public and political support for the CO_2-hyphotesis the 10 year warming period leading up to 1988 in all likelihood was important. Had the global temperature instead been decreasing, politic support for the hypothesis would have been difficult to obtain.

Based on the previous 10 years of concurrent temperature- and CO_2-increase, many climate scientists in 1988 presumably felt that their understanding of climate dynamics was sufficient to conclude about the importance of CO_2 for global temperature changes. From this it may safely be concluded that 10 years was considered a period long enough to demonstrate the effect of increasing atmospheric CO_2 on global temperatures.

Adopting this approach as to critical time length (at least 10 years), the varying relation (positive or negative) between global temperature and atmospheric CO_2 has been indicated in the lower panels of the diagrams above.

Last 20 year monthly surface air temperature changes, updated to December 2014
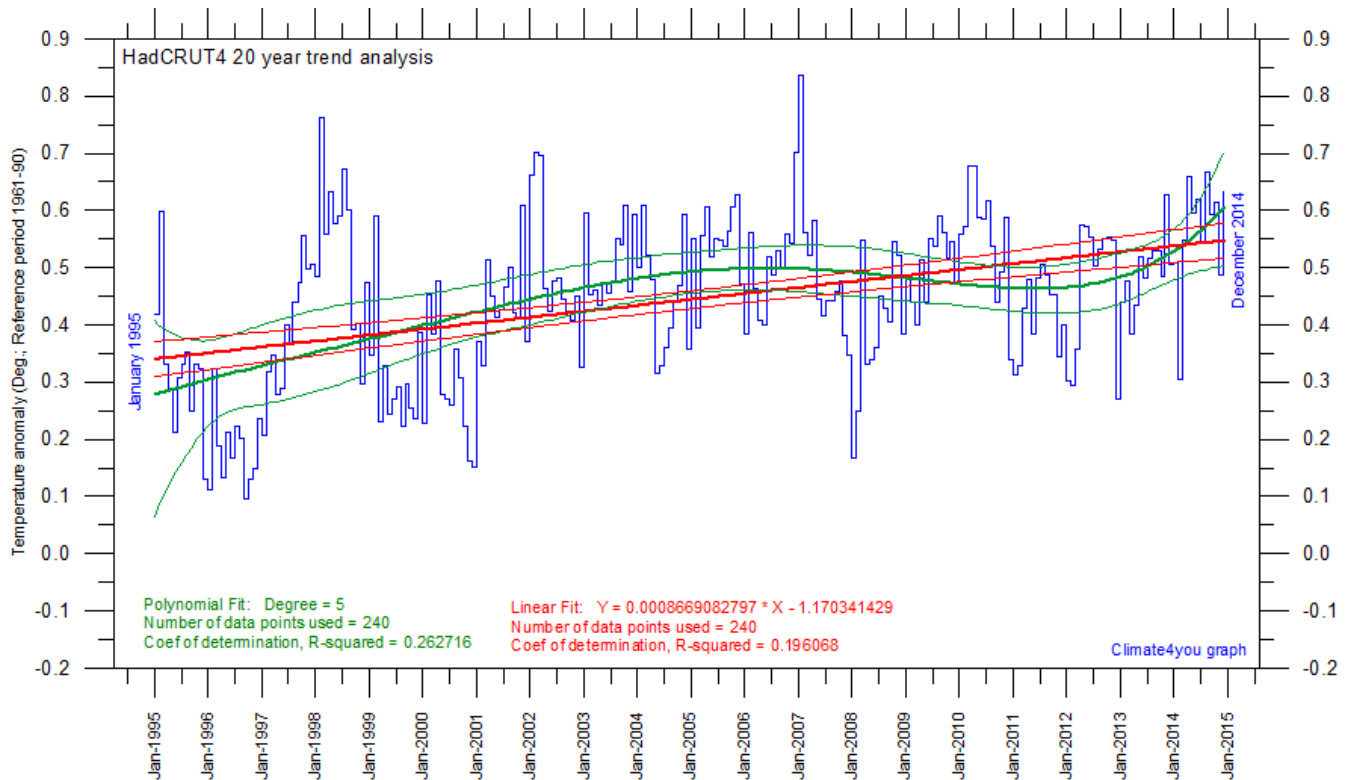
Last 20 years global monthly average surface air temperature according to Hadley CRUT, a cooperative effort between the Hadley Centre for Climate Prediction and Research and the University of East Anglia's Climatic Research Unit (CRU), UK. The thin blue line represents the monthly values. The thick red line is the linear fit, with 95% confidence intervals indicated by the two thin red lines. The thick green line represents a 5-degree polynomial fit, with 95% confidence intervals indicated by the two thin green lines. A few key statistics is given in the lower part of the diagram (note that the linear trend is the monthly trend). Please note that the linear regression is done by month, not year.

It is quite often debated if the global surface air temperature still increases, or if the temperature has levelled out during the last 15-18 years. The above diagram may be useful in this context, and demonstrates the differences between two often used statistical approaches to determine recent temperature trends. Please also note that such fits only attempt to describe the past, and usually have limited predictive power. In addition, before using any linear trend (or other) analysis of time series a proper statistical model should be chosen, based on statistical justification.

For temperature time series there is no *a priori* physical reason why the long-term trend should be linear in time. In fact, climatic time series often have trends for which a straight line is not a good approximation, as can clearly be seen from several of the diagrams in the present report.

For an excellent description of problems often encountered by analyses of temperature time series analyses please see Keenan, D.J. 2014: Statistical Analyses of Surface Temperatures in the IPCC Fifth Assessment Report.

1918: The "Spanish Flu" in Longyearbyen, Svalbard

The Longyearbyen cemetery on February 19, 2015, looking towards north. The graves for the seven Longyearbyen victims for the 'Spanish Flu' in October 1918 are marked by the nearest six wooden crosses and the single stone.

A serious outbreak of influenza occurred in the eastern United States of America in 1918, and rapidly developed into a pandemic spreading across the world from January 1918 to December 1920. Most influenza outbreaks disproportionately kill juvenile, elderly, or already weakened patients; in contrast the 1918 pandemic predominantly killed previously healthy young adults, typically in the 20 to 40 year age range.

Modern research, using virus taken from the bodies of frozen victims, has concluded that the virus kills through a cytokine storm (overreaction of the body's immune system). The strong immune reactions of young adults ravaged the body, whereas the weaker immune systems of children and middle-aged adults resulted in fewer deaths among those groups.

In early 1918 the 1st World War was still ongoing, and to maintain morale, wartime censors minimized early reports of illness and mortality in Germany, Britain, France, and the United States. However, newspapers were free to report the epidemic's effects in neutral Spain (such as the grave illness of King Alfonso XIII), creating a false impression of Spain as especially hard hit - thus the pandemic's nickname 'Spanish Flu'.

In remote Svalbard coal mining was ongoing in 1918 as coal was in high demand because of the 1st World War. In September 1918 the small mining community in Longyearbyen was hit by the pandemic, probably because of ships bringing new people and winter provisions from mainland Norway. Within few days' seven Norwegian miners, aged between 19 and 28, died of influenza within the first week of October 1918, and were buried in the small cemetery near Longyearbyen.

The identity of the 1918 'Spanish Flu' agent remains largely unknown, since human influenza virus was not known until 1933 (Smith, Andrews and Ladle 1933). Since then scientific interest in the type of virus

responsible for the 'Spanish Flu' has remained high, and burial sites with possible preservation of victims for the 1918 pandemic were looked for (Duncan 2006). Especially victims buried in Arctic regions were considered interesting, because of the high preservation potential due to permafrost.

An extensive search through death records of Arctic regions, for the last half of 1918, identified only few sites where the locations of the graves of victims of the 'Spanish Flu' were known (Duncan 2006). The most promising site was the cemetery in Longyearbyen (Davis et. al. 2000), as permafrost is known to be present all over Svalbard outside the extensive glacier cover. In 1997 an international group of experts was assembled by assembled by Canadian Dr. Kirsty Duncan, consisting of Norwegian, British, American and Canadian forensic experts, and receiving support from the Norwegian Church. The team obtained permission from the Norwegian authorities and family relatives to exhume six of the seven bodies buried October 1918 in Longyearbyen for sampling of remaining tissue.

In preparation for exhuming the 'Spanish Flu' victims buried in the Longyearbyen cemetery, a detailed geophysical survey of the grave site and its surroundings was carried out in 1997, to determine the precise horizontal location and vertical depth of the coffins, and the thickness of the active layer overlying the permafrost. The Longyearbyen cemetery itself is located on a SE facing slope, shortly outside the settlement, and is one of the first sites in the valley to receive direct sunshine in spring. All graves are marked with wooden crosses and a few stones, with the individual graves dug into a 2-3 m sediment layer (a glacial till) overlying solid bedrock below.

At the end of summer, the thawed active layer today typically is 1-1.5 m thick in the Longyearbyen area, depending on winter snow cover, vegetation, sediment type, soil moisture, slope aspect, topographic shading, etc. A Ground Penetrating Radar (GPR) was used for the survey, which was carried out in October 1997. Based on meteorological observations from Longyearbyen, Davis et al. (2000) in 1997 expected a maximum active layer thickness at the cemetery of 1.2 m since 1918.

The GPR survey demonstrated soil disturbances down to about 2 m depth. In Longyearbyen around 1918,

dynamite was often used to loosen the frozen soil for excavation, and this would account for the ground showing cone-shaped disturbances to at least 2 m below the terrain surface. By this there was reason to believe that the coffins with the seven Longyearbyen 'Spanish Flu' victims would have remained in permafrost since burial in October 1918, and that tissue with remnant virus could still be recovered.
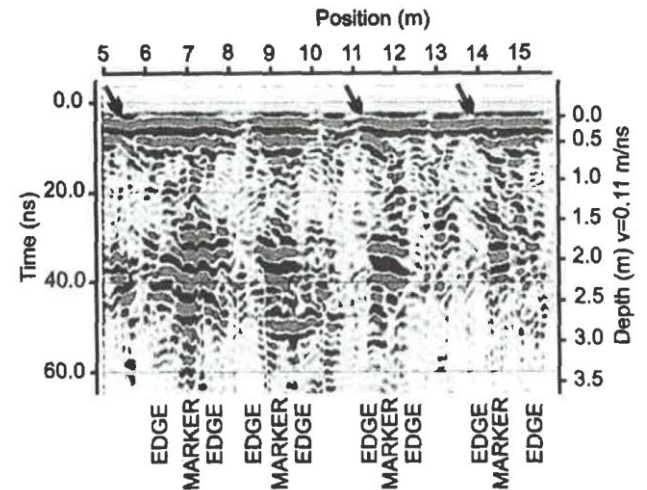
GPR profile across graves in the Longyearbyen cemetery. The diagram clearly shows disturbances of the original soil layering to about 2 m depth. Picture source: Davis et al. 2000.

The risk of exhuming living virus was considered high, and the excavations in 1998 were therefore carried out following strict safety measures. The excavations, however, rapidly demonstrated the real situation to be somewhat different from what was expected.

All coffins with the seven Spanish Flu victims were placed next to one another. Only one coffin was intact, whereas the others had collapsed and filled with soil. Most important, however, all coffins were at a depth of less than 1 m, and therefore not embedded in permafrost. Below the coffins the soil had clearly been loosened to a depth of 2 m as indicated by the GPR survey, but the coffins had nevertheless not been placed at this depth during the burial. Only little human tissue was therefore preserved at the time of excavation in 1998, but in fact enough to make analyses possible.
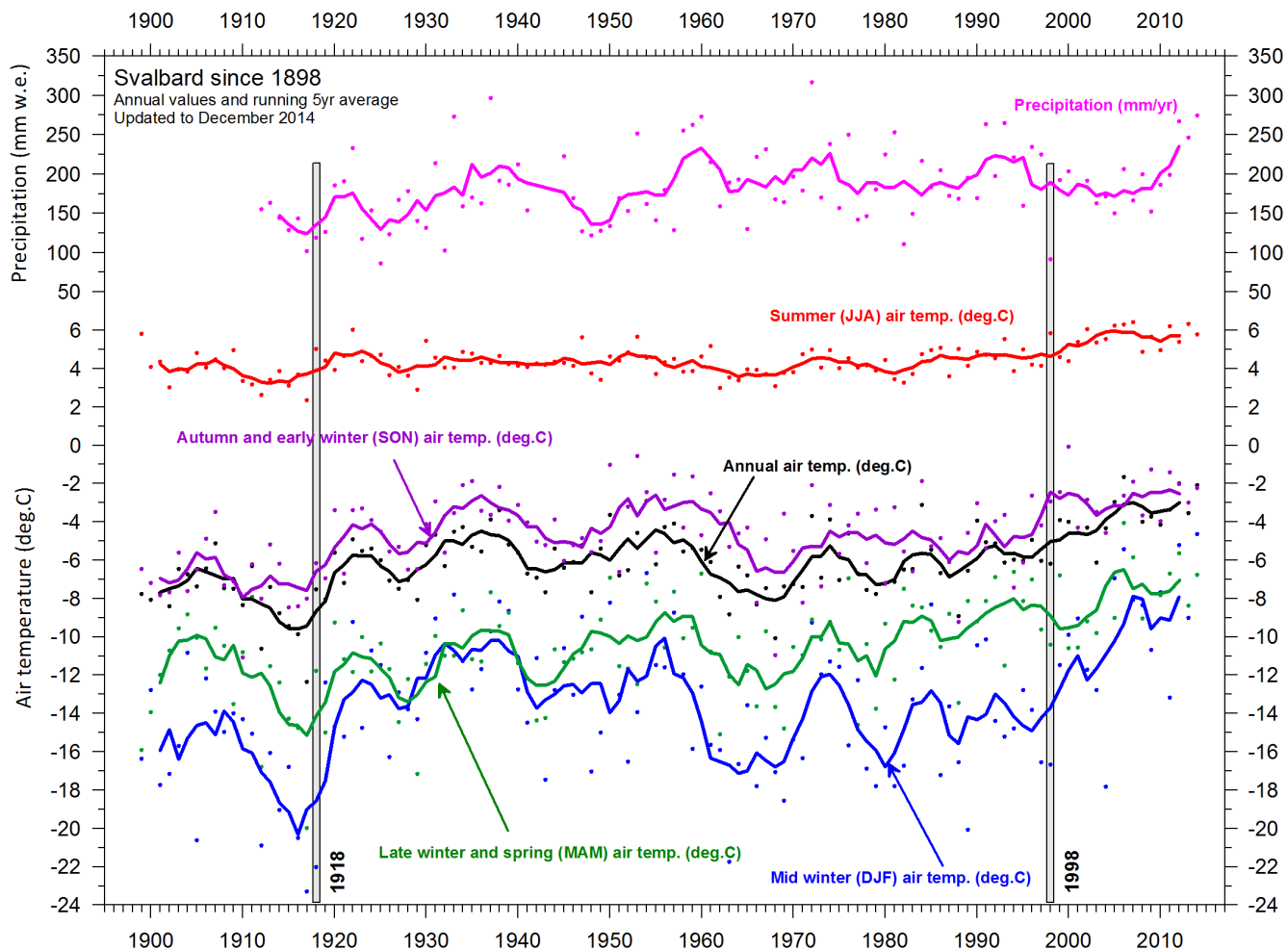
The composite Svalbard meteorological record (data from Nordli et al. 2014), with burial and excavation year, 1918 and 1998, respectively, indicated by grey bars. Please note that 1998 also marks the famous El Niño year.

The Svalbard meteorological series (see diagram above) provides part of the explanation why the coffins were not embedded in permafrost when excavated in 1998. In 1918 Svalbard was experiencing its version of the rapid Arctic warming 1915-1923, but conditions in 1918 were still relatively cold, compared to early 21st century conditions. In addition, the preceding period since 1908 represents a very cold period – actually the coldest within the entire Svalbard observational record.

Taken together, from this a shallow thawed active layer in 1918 may be inferred, and should the coffins at that time have been placed in the topmost part of the permafrost, chances are that the following warm periods culminating around 1938 and 1956 might have brought the coffins out of the permafrost and into the lowermost part of the active layer, by which the bodies would begin to decompose. The subsequent cold periods centred around 1965 and 1982 might partly have re-established permafrost around the lower part of the coffins, but this might have been too late to preserve the bodies.

A supplementary explanation for the failure to place the coffins with the Longyearbyen 'Spanish Flu' victims in permafrost was suggested by Davis et al. 2000.

The situation in Longyearbyen October 1918 was probably very unpleasant in several ways, to say it mildly. Presumably, the last ship before next spring had left at that time, and suddenly there was an outbreak of a serious decease in this small, isolated community. The decrease was spreading rapidly, killing even young and otherwise strong people, and there was no known cure. The persons responsible for the burial in October 1918 had to carry out their work in frozen soil, most likely in cold and unpleasant weather conditions, handling dead

bodies which apparently were carrying a highly contagious and potentially deadly decease. Not a very pleasant situation.

Small wonder should they on this background have decided to get the burial job done quickly, without spending much time to remove loose frozen soil to clear the holes left by the dynamite explosions to a greater depth than just about 1 m. A burial depth of 1 m was sufficient to get the coffins decently below the terrain surface, but certainly not very much into the permafrost.

What were the main forensic results of the international research team working at the Longyearbyen cemetery? In the best preserved of the Longyearbyen 'Spanish Flu' victims, fragments of virus were recovered from the lung, liver, kidney, and brain. Previously the virus had apparently only been found in lung tissue. This suggests that the disease on Svalbard may have gone systemic, attacking numerous organs, not just the lungs, as had previously been suspected.

References:

Davis et al. 2000. Ground Penetrating Radar Surveys to Locate 1918 Spanish Flu Victims in Permafrost. *Journal of Forensic Sciences* 45(1), 68-76.

Duncan, K. 2006. *Hunting the 1918 Flu. One scientist' Search for a Killer Virus*. University of Toronto Press, Toronto, Canada, 297 pp. ISBN 0-8020-8748-5.

Nordli, Ø., Przybylak, R., Ogilvie, A.E.J. and Isaksen, K. 2014. Long-term temperature trends and variability on Spitsbergen: the extended Svalbard Airport temperature series, 1898-2012. *Polar* Research 33, 23 pages, 21349, http://dx.doi.org/10.3402/polar.v33.21349

Smith, W., Andrews, C.H. and Ladle, P.P. 1933. Virus obtained from influenza patients. *Lancet* 225(ii), 66-8.

*****

All the above diagrams with supplementary information, including links to data sources and previous issues of this newsletter, are available on www.climate4you.com

Yours sincerely,

Ole Humlum (Ole.Humlum@geo.uio.no)

February 20, 2015.